Ocean Sci. Discuss., 9, 3127–3190, 2012
www.ocean-sci-discuss.net/9/3127/2012/
doi:10.5194/osd-9-3127-2012

Ocean Science Discussions

Recirculation in the Fram Strait and transports of water in and north of the Fram Strait derived from CTD data

M. Marnela[1,2], **B. Rudels**[1,2], **M.-N. Houssais**[3], **A. Beszczynska-Möller**[4], and **P. B. Eriksson**[1]

[1]Finnish Meteorological Institute, Helsinki, Finland
[2]University of Helsinki, Finland
[3]Laboratoire d'Océanographie et du Climat, Paris, France
[4]Alfred Wegener Institute for Polar and Marine Research, Bremerhaven, Germany

Received: 13 September 2012 – Accepted: 19 September 2012 – Published: 10 October 2012

Correspondence to: M. Marnela (marika.marnela@fmi.fi)

Published by Copernicus Publications on behalf of the European Geosciences Union.

Abstract

The volume, heat and freshwater transports in the Fram Strait are estimated from geostrophic computations based on summer hydrographical data from 1984, 1997, 2002 and 2004. In these years, in addition to the usually sampled section along 79° N, a section between Greenland and Svalbard was sampled further north. Quasi-closed boxes bounded by the two sections and Greenland and Svalbard can then be formed and conservation constraints applied on the boxes. The net volume flux is southward and varies between 2 and 4 Sv. The recirculation of Atlantic water is about 2 Sv. Heat is lost to the atmosphere and the heat loss averaged for the four boxes is about 10 TW and the net heat (temperature) transport is 20 TW northward into the Arctic Ocean, with large interannual differences. The mean net freshwater added between the sections is 40 mSv and the mean freshwater transport southward across 79° N is less than 60 mSv, indicating that most of the liquid freshwater leaving the Arctic Ocean through Fram Strait in summer derives from sea ice melt in the northern vicinity of the strait.

In 1997, 2001 and 2003 meridional sections along 0° longitude were sampled and in 2003 two smaller boxes can be formed, and the recirculation of Atlantic water in the strait is estimated by geostrophic computations and continuity constraints. The recirculation is weaker close to 80° N than close to 78° N, indicating that the recirculation is mainly confined to south of 80° N. This is supported by the observations in 1997 and 2001, when only the northern part of the meridional section, from 79° N to 80° N, can be computed with the constraints applied. The recirculation is found strongest close to 79° N.

1 Introduction

Fram Strait with a 2600 m sill depth is the most important passage between the Arctic Ocean and the Nordic Seas for oceanic transports of heat and freshwater and for sea ice (Fig. 1). On the eastern side of the strait the West Spitsbergen Current transports warm and saline water towards the Arctic Ocean. On the western side cold and low salinity surface water is transported southward by the East Greenland Current. The exchanges through the strait play an important role in the heat and freshwater budgets of the Arctic Ocean and have effects on the Arctic sea ice cover as well as on the meridional overturning circulation, which is, at least partly, responsible for the mild climate in the North-Western Europe. The exchanges through the strait have been monitored continuously by hydrographic observations and by direct current measurements since 1997 (Schauer et al., 2008), and irregularly for 30 yr. The dynamic nature of the exchanges, with strong boundary currents on both sides of the strait, time variability, intense baroclinic and barotropic eddy activity and substantial recirculation (e.g. Teigen et al., 2011), makes it difficult to accurately define and determine the transports between the Nordic Seas and the Arctic Ocean.

The geostrophic transports of volume/mass, heat and salt/freshwater through Fram strait have previously been computed from full hydrographic sections extending from Greenland to Svalbard with different approaches to determine the reference velocities by e.g. Palfrey (1967), Rudels (1987), Bourke et al. (1988), Schlichtholz and Houssais (1999). One recent attempt was made by Rudels et al. (2008), who dealt with the problem of the unknown reference velocity by applying constraints on the salt and volume transports in the deep waters and by evaluating the Arctic Ocean volume and freshwater balances.

The transports have also been estimated from direct current observations. First only in the West Spitsbergen Current (Aagaard et al., 1973; Aagaard and Greisman, 1975) and in the East Greenland Current (Foldvik et al., 1988) but later through a full section at 78°50′ N that has been monitored continuously since 1997 (e.g. Fahrbach et al., 2001; Schauer et al., 2004, 2008). However, in spite of the large number of moorings, the small scale features of the flow field are still not resolved and undersampling could lead to aliasing of the results and to large variations in the transport estimates.

A seasonal signal in the Fram Strait exchanges has been reported by e.g. Fahrbach et al. (2001) and Schauer et al. (2004) who note a minimum volume transport in

OSD
9, 3127–3190, 2012

the West Spitsbergen Current in summer with large monthly fluctuations. In the East Greenland Current the seasonal signal is less clear (Fahrbach et al., 2001; Schauer et al., 2004) although de Steur et al. (2009) find a summer minimum also in the East Greenland Current.

The exchanges through Fram Strait have also been estimated from models, e.g. Karcher et al. (2003), Maslowski et al. (2004), Karcher et al. (2008), and Fieg et al. (2010). The transports are similar or somewhat smaller than those obtained from direct current measurements and geostrophy. Fieg et al. (2010) find similar fluctuations as in the current meter array and no annual cycle in the net transport.

In this paper the exchanges of volume, heat and freshwater in the Fram Strait are estimated as well as the recirculation in the strait. The transports of volume, heat and freshwater through Fram Strait are obtained by computing the geostrophic transports through two CTD sections, one section located in Fram Strait at about 79° N and the second taken north of the strait extending from Svalbard to Greenland (Fig. 2). A set of conservation constraints are applied on volume, heat and salt for the boxes defined in the north and south by the CTD sections, to the east by the Svalbard slope and to the west by the Greenland slope. The undetermined reference velocities can then be estimated using a variational approach, without having to pre-define e.g. the net salt and volume transports in the deeper layers as was done in a previous study by Rudels et al. (2008).

Only few complete oceanographic sections have been occupied between Greenland and Svalbard north of Fram Strait beyond the recirculation area that can be combined with the 79° N section. (Figs. 2 and 3). The summers studied are 1984, 1997, 2002 (with one section taken in spring) and 2004. The exchanges of volume, heat and freshwater as well as the transports of different water masses are determined. The availability of two zonal (east-west) sections also makes it possible to estimate the summer ice melt in the Fram Strait as well as the local net heat loss in the area between sections. The heat and freshwater transport results are linked with atmospheric forcing to estimate their reasonability.

OSD
9, 3127–3190, 2012

The recirculation in the Fram Strait is not fully understood. The zonal section pair computations are also used to separate the recirculation in the Fram Strait from the exchanges between the Arctic Ocean and the Nordic Seas. The recirculation is computed more directly from north-south hydrographic sections located in the strait close to the Greenwich meridian (0° longitude) between 78° N and 80° N (Fig. 4). The sections are from summers of 1997, 2001 and 2003. Boxes closed by CTD sections on three sides and by the Greenland or Svalbard slope on one side are formed (Fig. 4) and geostrophic transports through the sides of the boxes are computed. The velocities are adjusted to fulfil volume, heat and salt conservation constraints.

In Sect. 2 the data are presented. In Sect. 3 the geostrophic transport computations as well as the different hydrographic sections and section pairs are described in detail. In Sect. 4 results are shown for volume, heat (temperature) and freshwater transports as well as for recirculation. Section 5 contains the discussion.

2 Data

CTD (conductivity (salinity), temperature and depth) data obtained during various cruises (Figs. 2 and 4) are examined. The east-west section pairs used are two Lance 1984 (18 July to 29 August) sections, a VEINS (Variability of Exchanges In the Northern Seas) section pair taken in 1997 with a northern Polarstern section (2 to 27 July) combined with a Lance section at 79° N (25 August to 7 September) and two Polarstern 2004 (17 July to 26 August) sections taken during the ASOF (Arctic Subarctic Ocean Fluxes) programme. A two-part Oden section in the north taken in 2002 (9 to 14 May) can also be used together with a Polarstern section at 79° N (31 July to 15 August) (Figs. 2 and 3). The north-south sections are from 1997 (24 August to 15 September) and 2003 (8 to 23 September) taken by Lance, and 2001 by Polarstern (23 June to 27 July).

For all years the data have been averaged for every 1 dbar except for 1997 Lance where the average is over 2 dbar. The data were extrapolated to the surface (0 dbar)

OSD
9, 3127–3190, 2012

by taking the values from the uppermost measurements and retaining these all the way to the surface. The instruments used were Seabird 911*plus* CTDs except in 1984 when a Neil Brown Mark III CTD was used. The CTD data, except 1984, have been processed using the Seabird software and the conductivity has been calibrated against water samples. The salinity error is about 0.003 except for the 1997 Polarstern cruise, where it might be as large as 0.005. The 1984 data had a drifting pressure sensor and the data had to be adjusted over time as well as calibrated against salinity samples. Unfortunately many of the calibration samples were destroyed as a geological sample was dropped on a salinity box. The error in salinity on the 1984 data could therefore be ±0.004. The 1984 data have been processed by removing instabilities through homogenising the underlying layer until static stability and the surface layer, 0 to 10 dbar, has been given the salinity and temperature values measured at 10 dbar.

Vessel mounted ADCP (Acoustic Doppler Current Profiler) data are available underway from the Polarstern 2004 cruise. The instrument is a narrow band 150 kHz ADCP from RD Instruments. The ADCP pings have been averaged within 1 min ensembles and 8 m bins. The velocity data used here have been de-tided using the AOTIM-5 model by removing all semi-diurnal and 4 diurnal tidal constituents (Padman and Erofeeva, 2004). The ADCP data were further averaged onto 10 min and 10 m cells and reach from 25 m to a maximum depth of 425 m.

Era-Interim Reanalyses, produced by the European Center of Medium-Range Weather Forecast (ECMWF) publicly available at http://data-portal.ecmwf.int/ are used to compute meteorological fluxes for 1984, 1997, 2002 and 2004. The data used are 12-h cumulative values of surface fluxes, at the spatial resolution of 0.75° (lat/lon). The wind fields in Fram Strait are also obtained from the ERA Interim Reanalyses.

Location of sea ice edge is visually estimated from the US National Snow and Ice Data Center's satellite based monthly sea ice concentration and extent images on Sea Ice Index (http://nsidc.org/data/seaice_index/) and also obtained from the ERA Interim Reanalyses.

OSD
9, 3127–3190, 2012

3 Method

3.1 Geostrophic computations

The geostrophic method assumes a balance between the Coriolis force and the pressure gradient. Geostrophic balance for the velocity component normal to the line connecting the CTD stations, or x-axis, can be written as

$$v \cdot 2\Omega \sin\varphi = -\frac{1}{\rho}\frac{\partial p}{\partial x} \tag{1}$$

where v is the velocity, Ω is the angular velocity of Earth ($7.292 \times 10^{-5}\,\mathrm{rad\,s^{-1}}$), φ is latitude, ρ is density and p is pressure. The geostrophic velocities between station pairs are first computed with zero velocity at the bottom of the shallower station of the pair. The method of Jacobsen and Jensen (1926) is then used for determining the velocities at the deeper station at all levels j located below the deepest common level of the station pair. This involves computing the difference between the specific volume anomaly of the bottom-most measurement of the shallow station i and the specific volume anomaly at the corresponding pressure of the deep station $i+1$. The velocity is then obtained by dividing the anomaly difference $\Delta\delta_i$ by the distance L_i between the stations and by Coriolis term f ($f = 2\Omega\sin\varphi$), and multiplying by a depth dependent sum. For layers j of thickness $\mathrm{d}h = 1\,\mathrm{dbar}$ (except $\mathrm{d}h = 2\,\mathrm{dbar}$ in 1997) below the shallow station, we get

$$v_{i+1,j} = \frac{\Delta\delta_i}{L_i f}\sum_{j=1}^{n}(\Delta H_i - j \cdot \mathrm{d}h)/\Delta H_i \tag{2}$$

where ΔH_i is the difference between the bottom depth of the deep station and the bottom depth of the shallow station and $n = \Delta H_i/\mathrm{d}h$ is the number of layers from the maximum depth of the shallow station to the maximum depth of the deep station.

OSD
9, 3127–3190, 2012

This represents the velocity for the deep station below the maximum depth of the shallow station. From direct current observations it is known that the currents in Fram Strait close to bottom tend to flow northward on the eastern slope and southward on the western slope. In the slope areas on all sections, the velocity is therefore set to zero either at the bottom of the shallow station or at the bottom of the deep station of the station pair. The choice is made in order to have the flow in the deep part, below the maximum depth of the shallow station, going in the direction indicated by the direct current observations, that is northward in the east and southward in the west. For the stations in the central parts, on the shelf areas and in Sofia Deep the velocity is kept at zero at the bottom of the shallower station. Conservation constraints are then applied on volume, heat and salt.

3.2 Determination of the barotropic velocity correction

3.2.1 Conservation constraints

Conservation constraints are formulated on closed boxes in a way similar to Houssais et al. (1995).

A maximum of 6 constraints are set on the transports through the CTD section sides of the boxes:

1) $$\iint_{\gamma 1} v^{\mathrm{b}}(x) S(x,z) \mathrm{d}x \mathrm{d}z = S_{\mathrm{w}} - \iint_{\gamma 1} v^{\mathrm{bc}}(x,z) S(x,z) \mathrm{d}x \mathrm{d}z = S_{\mathrm{cw}}$$

2) $$\iint_{\gamma 2} v^{\mathrm{b}}(x) \mathrm{d}x \mathrm{d}z = V_{\mathrm{m}} - \iint_{\gamma 2} v^{\mathrm{bc}}(x,z) \mathrm{d}x \mathrm{d}z = V_{\mathrm{cm}}$$

3) $$\iint_{\gamma 3} v^{\mathrm{b}}(x) S(x,z) \mathrm{d}x \mathrm{d}z = S_{\mathrm{m}} - \iint_{\gamma 3} v^{\mathrm{bc}}(x,z) S(x,z) \mathrm{d}x \mathrm{d}z = S_{\mathrm{cm}}$$

OSD
9, 3127–3190, 2012
Recirculation and transports in Fram Strait
M. Marnela et al.

$$4)\ \iint\limits_{\gamma 4} v^{b}(x)\theta(x,z)\mathrm{d}x\mathrm{d}z = \theta_{m} - \iint\limits_{\gamma 4} v^{bc}(x,z)\theta(x,z)\mathrm{d}x\mathrm{d}z = \theta_{cm}$$

$$5)\ \iint\limits_{\gamma 5} v^{b}(x)\mathrm{d}x\mathrm{d}z = V_{d} - \iint\limits_{\gamma 5} v^{bc}(x,z)\mathrm{d}x\mathrm{d}z = V_{cd}$$

$$6)\ \iint\limits_{\gamma 6} v^{b}(x)\mathrm{d}x\mathrm{d}z = V_{s} - \iint\limits_{\gamma 6} v^{bc}(x,z)\mathrm{d}x\mathrm{d}z = V_{cs}, \qquad (3)$$

where $v^{b}(x)$ is the depth-independent barotropic velocity, $v^{bc}(x,z)$ is the baroclinic velocity from the geostrophic computations. S is salt, θ heat and V volume. Subscripts stand for as follows: w = whole, m = middle, d = deep, s = Sofia Deep and c for constraint.

Constraint 1 is applied on the whole water column, γ_1, and requires that salt S_w, but not volume, is conserved in the whole box. This allows for input and removal of freshwater at the sea surface, e.g. by ice melt or freezing. The salinity of sea ice is here taken to be zero. The volume change caused by the melting or freezing sea ice is then allowed to leave or enter the box. Mainly melting is expected during the summer observation period. Because of the air-sea-ice interactions heat is not conserved. Constraints 2–4 are applied on the part of the water column, $\gamma_2 = \gamma_3 = \gamma_4$, excluding Sofia Deep, below and at the potential density (σ_θ) surface 28.06 and above the 2744 dbar pressure level. The upper boundary of this deep volume is assumed to be below the influence of the atmosphere and local convection. The isobar also intersects Yermak Plateau thus separating the Fram Strait proper from the Sofia Deep. The lower boundary is the bottom depth of the deepest station on the 79° N sections. Constraint 2 requires volume V_m, constraint 3 salt S_m and constraint 4 heat θ_m to be conserved within the above described part of the water column. Constraint 5 is applied below and at the 2744 dbar pressure level on the northern section, γ_5, and requires that volume V_d is conserved below and at 2744 dbar, preventing any net transport in the northern section deeper than the 79° N sections. Constraint 6 is applied below and at 750 dbar in the Sofia Deep, γ_6, and requires that volume V_s is conserved. The 750 dbar boundary is the approximate depth below which there is no direct exchange between the Sofia Deep and the Fram Strait proper because of the blocking effect of the Yermak Plateau.

3.2.2 The variational approach

A variational approach is then used to find the least energetic barotropic corrections needed to fulfil the constraints in a way similar to the method in Rudels et al. (2008). The barotropic velocity component v^b is computed by minimizing the kinetic energy of the barotropic part (not the total kinetic energy as in Rudels, 1987; Houssais et al., 1995) using the method of Lagrangian multiplyers:

$$\frac{\partial}{\partial v^b}\left\{\iint_{\gamma 1}\frac{1}{2}\left(v^b(x)\right)^2 \mathrm{d}x\mathrm{d}z + \lambda_1\left(\iint_{\gamma 1} v^b(x)S(x,z)\mathrm{d}x\mathrm{d}z - S_{\mathrm{cw}}\right) + \right.$$
$$\lambda_2\left(\iint_{\gamma 2} v^b(x)\mathrm{d}x\mathrm{d}z - V_{\mathrm{cm}}\right) + \lambda_3\left(\iint_{\gamma 3} v^b(x)S(x,z)\mathrm{d}x\mathrm{d}z - S_{\mathrm{cm}}\right) +$$
$$\lambda_4\left(\iint_{\gamma 4} v^b(x)\theta(x,z)\mathrm{d}x\mathrm{d}z - \theta_{\mathrm{cm}}\right) + \lambda_5\left(\iint_{\gamma 5} v^b(x)\mathrm{d}x\mathrm{d}z - V_{\mathrm{cd}}\right) +$$
$$\left.\lambda_6\left(\iint_{\gamma 6} v^b(x)\mathrm{d}x\mathrm{d}z - V_{\mathrm{cs}}\right)\right\} = 0 \quad (4)$$

Discussion Paper | Discussion Paper | Discussion Paper | Discussion Paper |
OSD
9, 3127–3190, 2012
Recirculation and transports in Fram Strait
M. Marnela et al.

which in discrete form can be written as:

$$\frac{\partial}{\partial v^{\mathrm{b}}}\left\{\sum_{i\in\gamma1}\frac{1}{2}(v_i^{\mathrm{b}})^2\sum_{j\in\gamma1}a_{ij}+\lambda_1\left(\sum_{i\in\gamma1}(v_i^{\mathrm{b}})\sum_{j\in\gamma1}a_{ij}s_{ij}-S_{\mathrm{cw}}\right)+\right.$$

$$\lambda_2\left(\sum_{i\in\gamma2}(v_i^{\mathrm{b}})\sum_{j\in\gamma2}a_{ij}-V_{\mathrm{cm}}\right)+\lambda_3\left(\sum_{i\in\gamma3}(v_i^{\mathrm{b}})\sum_{j\in\gamma3}a_{ij}s_{ij}-S_{\mathrm{cm}}\right)+$$

$$\lambda_4\left(\sum_{i\in\gamma4}(v_i^{\mathrm{b}})\sum_{j\in\gamma4}a_{ij}\theta_{ij}-\theta_{\mathrm{cm}}\right)+\lambda_5\left(\sum_{i\in\gamma5}(v_i^{\mathrm{b}})\sum_{j\in\gamma5}a_{ij}-V_{\mathrm{cd}}\right)+$$

$$\left.\lambda_6\left(\sum_{i\in\gamma6}(v_i^{\mathrm{b}})\sum_{j\in\gamma6}a_{ij}-V_{\mathrm{cs}}\right)\right\}=0 \tag{5}$$

where the sums are taken over the station halves i and depths $z(i,j)$ corresponding to the intervals from γ_1 to γ_6. The temperature θ_{ij} and salinity s_{ij} properties of each station are assumed to extend halfway to the neighbouring stations and a_{ij} is the area where the property is considered valid: half of the distance to the neighbouring CTD station multiplied by dh. The two halves of the same station are treated separately and different reference velocities can be added to them (Rudels, 1987). After derivation this results to:

$$a_i^1 v_i^b+\lambda_1 s_i^1+\lambda_2 a_i^2+\lambda_3 s_i^3+\lambda_4\theta_i^4+\lambda_5 a_i^5+\lambda_6 a_i^6=0 \tag{6}$$

where

$$a_i^k=\sum_{j\in\gamma k}a_{ij}$$

$$s_i^k=\sum_{j\in\gamma k}a_{ij}s_{ij}$$

OSD
9, 3127–3190, 2012

$$\theta_i^k = \sum_{j \in \gamma k} a_{ij} \theta_{ij}$$

and $k = 1 \ldots 6$

$$\text{i.e.} \quad v_i^{\text{b}} + \lambda_1 \frac{s_i^1}{a_i^1} + \lambda_2 \frac{a_i^2}{a_i^1} + \lambda_3 \frac{s_i^3}{a_i^1} + \lambda_4 \frac{\theta_i^4}{a_i^1} + \lambda_5 \frac{a_i^5}{a_i^1} + \lambda_6 \frac{a_i^6}{a_i^1} = 0 \tag{7}$$

$$\text{i.e.} \quad \boldsymbol{v}^{\text{b}} + \mathbf{B}\boldsymbol{\Lambda} = 0, \quad \text{where} \tag{8}$$

$$\mathbf{B} = \begin{bmatrix} \vdots & \vdots & \vdots & \vdots & \vdots & \vdots \\ \frac{s_i^1}{a_i^1} & \frac{a_i^2}{a_i^1} & \frac{s_i^3}{a_i^1} & \frac{\theta_i^4}{a_i^1} & \frac{a_i^5}{a_i^1} & \frac{a_i^6}{a_i^1} \\ \vdots & \vdots & \vdots & \vdots & \vdots & \vdots \end{bmatrix} \quad \text{and} \quad \boldsymbol{\Lambda} = \begin{bmatrix} \lambda_1 \\ \vdots \\ \lambda_6 \end{bmatrix}.$$

Solving Eqs. (8) and

$$\mathbf{A}^T \boldsymbol{v}^{\text{b}} = \boldsymbol{C}, \quad \text{where} \tag{9}$$

$$\mathbf{A} = \begin{bmatrix} \vdots & \vdots & \vdots & \vdots & \vdots & \vdots \\ s_i^1 & a_i^2 & s_i^3 & \theta_i^4 & a_i^5 & a_i^6 \\ \vdots & \vdots & \vdots & \vdots & \vdots & \vdots \end{bmatrix} \quad \text{and} \quad \boldsymbol{C} = \left[S_{\text{cw}} V_{\text{cm}} S_{\text{cm}} \theta_{\text{cm}} V_{\text{cd}} V_{\text{cs}}\right]^T$$

gives the barotropic velocity

$$\boldsymbol{v}^{\text{b}} = \mathbf{B}(\mathbf{A}^T\mathbf{B})^{-1}\boldsymbol{C} \tag{10}$$

and the new velocity becomes

$$v_{ij} = v_{ij}^{\text{bc}} + v_i^{\text{b}}. \tag{11}$$

The constraints are deliberately kept weak with only heat, volume and salt, but not water masses conserved. This allows for both isopycnal and diapycnal mixing between water masses. The reference velocities are determined by solving the Moore-Penrose inverse $B(A^T B)^{-1}$ with no error term introduced in the equations.

3.2.3 Choice of constraints

Zonal (east-west) sections

Geostrophic transports are computed for the 1984, 1997, 2002 and 2004 east-west section pairs, where one section is located in Fram Strait at about 79° N and the second farther north, between 80° N and 83° N (Fig. 2). It is assumed that all water exchanged through Fram Strait passes through the two sections and that reasonable constraints can be formulated for the box enclosed by the sections and by Greenland and Svalbard.

The 2004 Polarstern cruise does not cross Sofia Deep and constraint 6 is not required. For the other years all 6 constraints are required.

The 1997 Polarstern cruise north of Fram Strait is combined with the Lance cruise at 79° N (1 month between the cruises). Since the Lance 79° N data are averaged over 2 dbar, whereas the Polarstern data are averaged over 1 dbar, the velocities are computed for every dbar on the northern Polarstern section and when the sections are put together only every second value, corresponding to those obtained for the 79° N section, is used to simplify the combination of the sections.

The 2002 Oden sections north of Fram Strait are combined and used together with a Polarstern section at 79° N taken two months later. A gap exists between the western and eastern Oden section and these sections were therefore treated separately in a previous transport estimate (Marnela et al., 2008) (Fig. 2). The eastern section was given zero velocity at the surface by them. Here the sections are combined and the initial velocity is set to zero at the bottom (see above). An additional problem here is that the first two stations west of the gap only reach 1200 m, which compromises the conservation constraints.

Meridional (north-south) sections

Geostrophic transports are computed for the 1997, 2001 and 2003 north-south sections in Fram strait at 0° longitude between 78° N and 80° N to get a better estimate of the recirculation in Fram Strait. Two boxes can be formed in 2003. The northern box is closed by the Svalbard slope in the east and by three CTD sections, one in the west along 0-meridian and the others along 78.8° N and along about 80° N. The southern box is closed by the Greenland slope in the west and by three CTD sections, one in the east along 0-meridian and the others along 78° N and 78.8° N. Only the northern box can be formed in 1997 and 2001, as shown in Fig. 4.

Three constraints, 2 to 4, are applied for the deep part below potential density 28.06, allowing no volume, salt or heat to accumulate in the deep part. The shallower stations on the slopes are less dense than 28.06 and the constraints are not applied to them nor are the stations included in the minimization. For the computation of the recirculation across the 0° longitude this should give a reasonable estimate since all the stations here are deep. Two of the 2003 stations, however, do not reach to the bottom in the along-0-meridian part of the southern box.

4 Results

4.1 Volume transports and recirculation

4.1.1 Transports from zonal section pairs

The net volume transports through the Fram Strait computed from the baroclinic velocities obtained from the hydrographic sections (Fig. 3) with velocity set to zero at the bottom and with no constraints applied are estimated to 4.5 Sv southward through the northern section and 2.9 Sv southward through the 79° N section averaged over the four east-west sections (Table 1).

The net volume transport through Fram Strait with the constraints applied is estimated to 3.1 Sv southward averaged over the four east-west section pairs. The transports are about 2 Sv for 1984 and 2004, and 4 Sv for 1997 and 2002 (Table 2). The

OSD
9, 3127–3190, 2012

mean total northward flow at 79° N is about 8 Sv, and at the northern section 5 Sv. The southward flow is 11 Sv at 79° N and 8 Sv at the northern section (Fig. 5, Table 2).

The transports of different water masses are also computed. Here we use the simplified water mass classification with six water masses introduced by Rudels et al. (2008). The water masses are separated by isopycnals except in the intermediate layer where both the dense Atlantic Water (dAW) and the Intermediate Water (IW) occupy the same density interval but are separated by the 0 °C isotherm (Table 3). The fluxes of the different waters are show in Fig. 6 in θS diagrams, where the θS properties of the transport of each water mass for each section and year are given by the positions and colours of the circles while the size of the circles indicates the volume transports.

The main net southward transports occur in the surface layer, where the low salinity cold Polar water is exported, and in the intermediate density range (dAW and IW), where the net outflow is close to 2 Sv in all years. This is in agreement with Rudels et al. (2008). These two outflows reflect, in the upper part, the river runoff and net precipitation, and the input of freshwater and low salinity Pacific water to the Arctic Ocean, and in the lower part, the water entering the Arctic Ocean over the Barents Sea.

The differences in water mass properties between the sections as well as between northward and southward flow through a section show that waters in the upper part, surface water and AW, coming from the south, become colder between the two sections. Atlantic water also becomes less saline, whereas surface water only becomes less saline in 1984 and 1997, and more saline in 2002 and 2004 (Table 4, Fig. 6).

At the upper levels the waters from the north become warmer between the northern and southern sections, but while the Surface water becomes less saline, except in 1984, reflecting ice melt between the sections, the Arctic Atlantic Water (AAW) becomes more saline indicating mixing with recirculating AW.

At the deeper levels the intermediate (below 0 °C) and deep waters from the north (light blue spots in Fig. 6) are warmer and more saline than the corresponding waters from the south (red spots in Fig. 6) and in general the waters from the north become

OSD
9, 3127–3190, 2012

colder and less saline and the waters from the south warmer and more saline as they pass through the strait (Fig. 6, Table 4). The differences in temperature become smaller in the 2000s as the Nordic Seas deep waters, the colder of the deep waters, have gotten warmer.

4.1.2 Recirculation

The recirculation can also be estimated from the east-west sections. Here it is defined as northward transport through 79° N section minus northward transport through the northern section. The recirculating surface and Atlantic waters become colder and less saline (Fig. 6). In 1984 2.6 Sv is estimated to recirculate in the strait, in 1997 no recirculation was found, in 2002 6.9 Sv and in 2004 2.6 Sv. The amount of AW recirculating is about 2 Sv except in 1997. The deepest water mass recirculates towards north by 0.5 Sv in 1997 and 2004.

The recirculation in the strait is larger than the net southward volume transport, except in 1997, and about 25 % of the water flowing southward through 79° N is estimated to be recirculating water returning to the south. Of the Atlantic water entering the strait from the south almost 50 % recirculates.

The westward recirculation between 78° N and 80° N in 2003 is estimated from the meridional sections to 2.3 Sv with 1.2 Sv between 78–78.8° N and 1.1 Sv between 78.8–80° N, when two closed boxes can be formed. The transport of recirculating Atlantic water is 1.2 Sv, with 0.7 Sv between 78–78.8° N and 0.5 Sv between 78.8–80° N, and of dense Atlantic water 0.7 Sv with 0.4 Sv and 0.3 Sv respectively (Table 5).

In 1997 and 2001 it is not possible to form both a northern and a southern box covering the 0° meridian from 78° N to 80° N, but only the northern box whose western section reaches from 78.8° N to 80° N. In 1997 the net transport between 78.8° N and 80° N is 0.7 Sv westward and of this, the transport of AW is 0.4 Sv and of dAW 0.2 Sv. In 2001 the net flow between 78.8° N and 80° N is 0.2 Sv eastward and the net transport of AW is westward by 0.06 Sv and that of dAW is 0.02 Sv eastward.

OSD
9, 3127–3190, 2012

The transports through a north-south section extending from 78° N to 80° N are also computed with the velocity set to zero at the bottom and with no constraints applied (Table 6). The transport for 2003 is estimated to 2.3 Sv westward. This volume transport is separated into 1.1 Sv through 78° N to 78.8° N and 1.2 Sv westward through 78.8° N to 80° N. From the 1997 section between 78° N and 80° N the transport for 1997 is estimated to 1.3 Sv westward. This volume transport is divided almost equally between 78° N to 78.8° N and 78.8° N to 80° N. The transport for 2001 is estimated to 0.4 Sv westward with 1.0 Sv westward between 78° N and 78.8° N and 0.6 Sv eastward between 78.8° N and 80° N (Table 6).

4.1.3 Volume transports from vessel mounted ADCP data

Vessel mounted ADCP data are available from the Polarstern 2004 cruise. The largest ADCP velocities from the 2004 cruise are found at the 78°50′ N section. On the eastern side of the strait there are rather regular fluctuations in the direction (south-westward and north-westward) and on the western side the direction is mainly south to south-westward. Northward transports are mainly confined to the eastern side of the sections (West Spitsbergen Current), in the northern section the strongest northward flow is seen on the western flanks of Yermak Plateau, at about 82° N, 7° E. Southward flow can be seen on the western side (East Greenland Current), but also as fluctuations along the 79° N section (Fig. 7).

The ADCP data are used to compare the direct current measurements from the ADCP with the geostrophy derived velocities. The ADCP data for the computations are selected corresponding to the center points of where the geostrophic velocities with constraints applied are thought to be valid, i.e. between two neighbouring CTD stations at 1/4 and 3/4 of the in-between distance. ADCP velocities are averaged over an area within ±0.1° in longitude and ±0.02° in latitude to these points. Both the ADCP and geostrophic velocities are averaged over a 35–55 m layer representing the surface water and over a 155–255 m layer representing the Atlantic water layer. The depth-independent differences between the geostrophic velocity and the ADCP velocity component normal to the line connecting the CTD stations are then added to the geostrophic velocities of the corresponding water masses to obtain an ADCP referenced velocity (see water mass definitions in Table 3). The correlation between the ADCP mean velocities and geostrophic mean velocities is at the 79° N section 0.75 for surface water layer and 0.63 for Atlantic water layer, but in the northern section there is no correlation for either water mass.

The results from the ADCP referenced geostrophy give net southward transports of both surface water and Atlantic water through both sections. The net surface water volume flow is 1.5 Sv southward through the 79° N section and 1.2 Sv through the northern section. The net Atlantic water volume flow is 1.8 Sv southward through the 79° N section and 1.6 Sv southward through the northern section. A gap in the stations at the 79° N section at about 5° E misses a substantial part in the geostrophy of the southward flow visible in the ADCP measurements (Fig. 7).

The ADCP transports are also computed for a 35 to 425 m layer, where ADCP mean is taken every 0.25°. At 79° N 5.5 Sv is found to flow northward and 7.1 Sv southward (net 1.6 Sv southward). Divided between western and eastern parts of the strait, to the west of the 0° meridian the transports are 1.6 Sv northward and 3.8 Sv southward, and to the east 3.8 Sv northward and 3.3 Sv southward. Through the northern section the transports are 1.3 Sv northward and 2.0 Sv southward (net 0.7 Sv southward) (Table 7).

From geostrophy the transports for a 35 to 425 m layer are at 79° N 4.2 Sv northward and 4.5 Sv southward. West of 0° E the transports are 1.5 Sv northward and 2.8 Sv southward, and east of 0° E 2.8 Sv northward and 1.7 Sv southward. Through the northern section the net transport is 0 Sv with 2.3 Sv both northward and southward (Table 7).

OSD
9, 3127–3190, 2012

4.2 Heat and freshwater transports

4.2.1 Reference temperature and salinity

The choice of reference temperature and salinity used to estimate the heat and freshwater transport is largely arbitrary and will, since there is a net southward volume transport through Fram Strait and hence no mass balance, affect the heat and freshwater flux estimates between the Nordic Seas and the Arctic Ocean. Often the term temperature flux is used instead of heat flux in situations where a net volume transport occurs. Traditionally the heat transports into the Arctic Ocean have been computed relative to −0.1 °C and the freshwater fluxes relative to 34.8 taken as the mean temperature and mean salinity of the Arctic Ocean water column (Aagaard and Greisman, 1975; Aagaard and Carmack, 1989; Dickson et al., 2007). Whether or not it was possible to determine an adequate mean temperature and salinity of the Arctic Ocean at that time is questionable. It is also likely that the mean temperature and salinity would have changed in 40 yr considering the reported variability of the inflow temperature and salinity and the increased temperature observed in the Atlantic layer in the Arctic Ocean (Quadfasel et al., 1991; Carmack et al., 1995; Polyakov et al., 2005; Beszczynska-Möller, 2012).

Rudels et al. (2008) used, when working on single sections, variable reference temperatures and salinities. The mean outflow temperature and the mean inflow salinity respectively were computed for each section and used as reference values for that section. The choice made the outflow carry no heat and the inflow carry no freshwater and the fluxes were then closely connected to the actual situation in Fram Strait during the observation time. Here, with two sections, the heat and freshwater fluxes for each year are computed relative to the mean temperature and mean salinity of the total transports into and out of the box. This choice again relates the heat (temperature) transport to the waters present at the actual time of the observation and also gives a possibility to relate the variations of the temperature and freshwater transports to the variations of the mean salinity and temperature of the waters present (Tables 2 and 3).

OSD
9, 3127–3190, 2012

The choice diminishes the effect of the violated mass conservation by keeping the reference temperature (salinity) close to the mean temperature (salinity) of the exchanged waters. This minimises the effect of the mass (im)balance since the excess mass flux has temperature (salinity) close to the reference temperature (salinity).

4.2.2 Results

Heat and freshwater transports (Fig. 5) are computed for the east-west section pairs relative to the mean temperature and the mean salinity of the total volume transport (Tables 2 and 4). The transports of heat and freshwater would be the same through both of the sections if there was no exchange with the atmosphere and with sea ice. For all four years there is net heat transport into the box and freshwater transport out of the box. To melt ice equivalent to the net freshwater divergence from the area between the sections

$$m_{fw} = \rho_w \cdot V_{fw}$$

where ρ_w is the density of sea water and V_{fw} is the volume of freshwater, the heat needed is

$$Q = \Delta H_{fus} \cdot m_{fw}$$

where $\Delta H_{fus} = 3.33 \times 10^5\,\mathrm{J\,kg^{-1}}$ is the latent heat of fusion of water.

In 1984 (37 mSv) this gives $Q = 13\,\mathrm{TW}$ (Table 8a). In 1984 the lateral convergence of heat, i.e. the ocean heat loss in the area between the sections, is 25 TW. This is more than enough to explain the increased amount of freshwater due to melting. In 1997 the net freshwater input of 8 mSv would require a heat input of 3 TW and 5 TW are provided by the ocean. In 2002 the freshwater imbalance is 58 mSv, which demands a heat input of 20 TW but only 14 TW is lost by the ocean. In 2004 the imbalance is 61 mSv, corresponding to a heat input of 21 TW, but only 2 TW are lost by the ocean between the sections.

OSD
9, 3127–3190, 2012

Year 2004 is studied in more detail, and it is first estimated whether the additional 19 TW of the heat needed to melt the ice corresponding to the net freshwater divergence could be added from the atmosphere and the radiation. From the ERA Interim data the atmospheric heat input integrated over two months (July, August) is 16 TW for an area located between the sections, from a spatial resolution of 0.75°, (latitude 79.5 to 82.5° N, and longitude 12° W to 9.75° E). This could melt 47 mSv of ice, which is in the same order of magnitude as the 61 mSv of freshwater estimated to leave the area. With the additional ice melt of 7 mSv from the heat lost by the ocean, the ice melt occurring in the strait based on geostrophic computations is nearly explained. In the other years the atmospheric heat input for the areas between the sections during July–August are: 1984 12 TW, 1997 11 TW and 2002 16 TW (between May–August 13 TW).

The freshwater input from total precipitation is also estimated. Evaporation is small. The cumulative precipitation and evaporation from ERA Interim data are integrated over time (July–August) and amount to 0.062 m per unit area in 2004. The net precipitation minus evaporation for an area between the two sections is thus $1.0 \times 10^{10}\,m^3$. This amount equals to 1.9 mSv, about 3 % of the estimated freshwater transport in 2004 (Table 8b). Adding this to the above computed values of atmospheric ice melt (47 mSv) and oceanic ice melt (7 mSv) gives 56 mSv as compared to the 61 mSv from geostrophy. The other years are presented in Table 8.

There is no reason to expect a balance between oceanic heat loss and ice melt, and these estimates only show that the heat loss is compatible with the sea ice melt between the sections. Less than half of the study area was ice-covered at the end of the measurement period.

The heat and freshwater transports are computed with variable reference temperature and salinity values. The transports were also computed relative to temperature −0.1 °C and to salinity 34.8, as well as relative to salinity 34.9, which has been used by various authors e.g. Holfort et al. (2008), de Steur et al. (2009) for Fram Strait

OSD
9, 3127–3190, 2012

computations. The net heat and freshwater transports through the strait thus obtained are almost the same regardless of the reference value.

The mean heat loss from the ocean between the two zonal sections can be estimated to 11 TW. About 30 % of the heat transported northward through the 79° N section is lost between the sections. The mean net freshwater transport southward through 79° N is from varying reference salinities 57 mSv and 15 mSv through the northern section. Using reference salinities of 34.8 and 34.9 we get 66 and 75 mSv across 79° N and 25 and 34 mSv through the northern section. The freshwater addition from the area between the sections thus is 40 mSv.

5 Discussion

5.1 Comparison of transport estimates from different methods

5.1.1 Northward and southward transports

We have estimated the transports and the recirculation in Fram Strait for 1984, 1997, 2002 and 2004 as well as the transports through 0° meridian between 78.8° N and 80° N for 1997, 2001 and 2003 from closed boxes, and for 2003 also between 78° N and 78.8° N. The transports through 0° meridian were also computed for 1997, 2001 and 2003 between 78° N and 80° N with no constraints applied.

The mean net volume transport through Fram Strait based on the four zonal section pairs is estimated to 3.1 Sv southward. In order to compare the present results with the results of Rudels et al. (2008), who obtained a mean transport of 2.7 Sv before using budget considerations that brought the net transport down to 1.7 Sv (Table 9), the transports are computed for a smaller section from the Greenland shelf break to the Svalbard shelf break at 79° N, i.e. from 6° W to 9° E. This gives a somewhat smaller estimate of 2.7 Sv southward. About 0.5 Sv was expected to flow southward on the Greenland shelf by Rudels et al. (2008) and that seems to be reasonable also from the present estimates (Tables 2 and 9, Fig. 1). Recent modelling results by Fieg et al. (2010), give an 11-yr mean net volume transport of 2.0 Sv southward through Fram Strait.surface. The instruments used were

The 2002 results are also compared with Oden results obtained by Marnela et al. (2008) using the northern section. They obtained 3.6 Sv northward on their eastern section and 5.1 Sv southward on the western section and 0.5 Sv northward between sections. Adding these values up gives a southward transport of only 1 Sv through the northern section as compared with the 4.1 Sv obtained here. For the less wide section that Rudels et al. (2008) used for the section at 79° N 3.4 Sv is here found, which is slightly less than the 3.6 Sv presented by Rudels et al. (2008).

Using a similar method for 1984, Houssais et al. (1995) obtain a net southward transport of 1.6 Sv whereas here we find 2.2 Sv southward. The differences are larger in the transports of individual water masses. Both get the same amount of freshwater, 40 mSv, added between the sections. Houssais et al. (1995) also suggest that their 0.7 Sv of Atlantic water converging in the area might be diluted by Polar surface water but the results presented here suggest that the 0.7 Sv of AW converging in the area could be mixed with the intermediate waters below.

Also the transports through 79° N can be computed for 2003 from the meridional section boxes. With constraints applied the net volume transport across 79° N is 3.1 Sv southward. This is close to the 3.3 Sv obtained by Rudels et al. (2008) from the same Lance data. The 2003 Polarstern section taken less than one month later than the Lance section gave a transport of 1.4 Sv southward (Rudels et al., 2008). Temporal variance this large is possible, as seen in the net volume flow from mooring data and also captured by the models (Fieg et al., 2010, Fig. 9), that however go in the opposite direction during the same time interval.

For 1997 and 2001 only the fluxes through the part of the 79° N section east of 0° longitude can be computed with constraints applied, the corresponding transports are 0.4 Sv and 0.7 Sv northward as compared with the 1.2 and 2.0 Sv northward from the

OSD
9, 3127–3190, 2012

method used by Rudels et al. (2008). From the zonal section pairs with constraints applied the transport for 1997 on the eastern side of the 79° N section is 0.7 Sv northward.

5.1.2 Recirculation

From the meridional section computations with and without constraints applied the results between 78.8° N and 80° N are of the same order and direction. The westward recirculation between 78.8° N and 80° N is largest in 2003.

For 1997 no recirculation was found from the zonal section pair, but from the meridional section a recirculation of 1.3 Sv westward was obtained. The data in the 1997 northern section are sparse and aliasing is likely to occur.

5.2 Sources of error

5.2.1 Data

Most of the data have not been smoothed. However, since the geostrophic computations integrate the density field, smaller disturbances tend to cancel out. Some spikes have been removed by linear extrapolation, but the data sets still contain small spikes, e.g. the 2003 Lance data for the northern box has a probable salinity spike of 0.004 present at a couple of stations. Such a spike perturbs the velocities by about $1 \times 10^{-5}\,\mathrm{m\,s^{-1}}$, which then affects the water column above the spike since the velocities are first set to zero at the bottom. The transport estimate assuming the distance between stations to be 20 km and depth 1 km above the spike, amounts to a missed volume of 0.2 mSv. This difference is small enough to be ignored.

The data close to the surface often are of poor quality. The largest depths that have been extrapolated to the surface by using constant values are on a station in 2001 from about 70 dbar to the surface, and in 2003 on a station from 29 dbar to the surface.

The location and length of the northern section vary from year to year sometimes crossing the Yermak Plateau and sometimes not. The 1997 and 2002 sections are

OSD
9, 3127–3190, 2012

taken over 2 months apart and hence not synoptic considering the variation in the strait. Also aliasing due to too few stations may occur.

5.2.2 Method

We have assumed that the transports not observed in the strait, because of the sections not reaching the coasts, are about equal on both sections and cancel out, and that the net flow passing one section also has to cross the other section, apart from the added ice melt. No heat or salt is allowed to accumulate in the deep part of the box during that time. These are assumptions. Rudels et al. (2008) estimated up to 1 Sv of water on the Greenland shelf passing southward beyond the standard 79° N section. Also on the eastern side of the strait there are transports between the coast and the easternmost station.

The velocities between stations cannot be readily deduced from the density field close to the bottom due to the non-uniform topography. The method of Jacobsen and Jensen used to estimate the velocities at the bottom of the deeper station in a station pair only takes into account the difference between the station properties at the bottom depth of the shallower station and the velocity for the deep station close to bottom is extrapolated linearly from that single difference.

Having the geostrophic velocity set to zero at the bottom without applying constraints leads to convergences between the zonal sections and imbalances with net inflows into the box ranging from 0.5 Sv in 1997 to 3.5 Sv in 1984 and a net outflow (divergence) of 0.7 Sv in 2002 (Table 1).

It is clear that the transports are highly dependent on the constraints (Table 10) used as well as on the available stations that form the section. The 1984 result is tested for aliasing by removing one station from the data. Although the net transport changes very little, up to about 0.1 Sv, the northward and southward transports can both differ by 2 Sv. Although the removal of a station from the section does not affect the net transports much, it can have large impacts on the individual northward and southward transports.

The depth of about 2700 m (2744 dbar) is used to block the deeper waters in the northern section from crossing the strait. However, the sill depth is cited as 2600 m in literature and studies of the bottom bathymetry in the Fram Strait show a very complex structure (e.g. Klenke and Schenke, 2002). We have on the 79° N sections 1–7 stations that reach deeper than 2600 m. Should we use that as a limiting depth, we would need an extra constraint for the deep part of the 79° N section assuming that the sill is at its shallowest between the sections. This is tested with the 2004 data and results give nearly the same transport of volume than what is computed here, difference between the results being less than about 2 %, except for the deep waters and AW. The largest differences are in the order of 0.1 Sv. The freshwater produced between the sections increases by 0.5 mSv. Heat/temperature seems to be the most sensitive of the three variables showing an increase of 23 % (0.5 TW) of heat lost between the sections. Mainly the difference is due to the more positive fluxes (warm Atlantic waters northward and cold deep water southward) at 79° N section.

5.2.3 Strait dynamics

There are eddies in Fram Strait and its vicinity, typically of diameter of 20–40 km with persistence time of 20–30 days (Johannessen et al., 1987; Quadfasel et al., 1987). Mesoscale eddies are an important mechanism by which AW may be recirculated from the WSC (Gascard et al., 1988; Schlichtholz and Houssais, 2002). These eddies may be missed by the hydrographic sections or misinterpreted due to aliasing e.g. if only one side of eddy is measured.

The recirculation may be located east of the 0° meridian and that part would be missed in the north-south sections.

With the constraints applied the convergence or divergence of a specific water mass in the box can be up to 0.5 Sv or more. The maximum convergence, 0.7 Sv, was found for AW in 1984 and the maximum divergence, 0.9 Sv, for the surface water in 2004 (Table 4). This indicates that diapycnal mixing occurs between the sections and affects a substantial fraction of the water masses as is seen from the θS volume diagram in

OSD
9, 3127–3190, 2012
Recirculation and transports in Fram Strait
M. Marnela et al.

Fig. 6. The main mixing is isopycnal as can be seen from the transformations of the water masses between the waters entering and leaving the boxes. The temperature-salinity shifts are mainly isopycnal.

The salinity of multi-year ice is about 2–3 psu and a little bit more in the first year ice at the end of summer and again slightly more at the beginning of the summer (Untersteiner, 1961). The salt contained in the sea ice crossing the box borders is not considered in the computations, but the salt released to the area between the zonal sections by melting is present in the data causing a small error less than 0.01 Sv in volume transports and about 0.01–0.03 mSv in freshwater transports (estimated assuming 4 psu sea ice).

The daily mean winds at 10 m height are obtained from the Era-Interim Reanalyses of ECMWF. The Ekman transport of water near the surface can be estimated from the data. Using the daily mean winds gives Ekman transports up to 0.5 Sv during the measurement periods, however, these transports nearly cancel out during the whole lengths of the period being ±0.005 Sv. The Ekman transports are considered small and not included in the computations.

6 Summary and conclusion

The mean net volume transport for the observed four years having velocity set to zero at the bottom and with no constraints applied is through the 79° N section 2.9 Sv southward and through the northern section 4.5 Sv southward, with an imbalance of 1.6 Sv between the sections. Applying the constraints changes the transport to 3.1 Sv and reduces the imbalance between the sections to less than 0.1 Sv. The net volume transports obtained from applying the constraints fall between the volume transports at the two sections with no constraints applied, i.e. the net volume transports increase at the 79° N section and decrease at the northern section except in 2002 the opposite. The sections in 2002 are exceptional in that the southward net transport without constraints is larger at the 79° N section than at the northern section. This is only partly explained

OSD
9, 3127–3190, 2012

by the extending of the section at 79° N furthest to the west in 2002, the flow estimated for the shelf part being 0.7 Sv (Fig. 2, Tables 1 and 2). The transport southward through the northern section is smallest in 2002. However, a gap with no observations between 1200 m and the bottom exists on the northern section (see Fig. 3).

The individual northward and southward volume fluxes are smaller than those obtained by direct current measurements (e.g. Schauer et al., 2008), but the net transports are of the same order, perhaps larger. If correct, this would require a larger inflow over the Barents Sea than the slightly above 2 Sv that has previously been estimated (e.g. Smedsrud et al., 2010) or a smaller outflow through the Canadian Arctic Archipelago than the 2 Sv given in most references (e.g. Melling et al., 2008). Recent results (e.g. Skagseth et al., 2011) find 3 Sv inflow to the Barents Sea.

The recirculation of AW in Fram Strait is estimated to about 2 Sv from both the east-west and north-south sections. The recirculation of intermediate waters is smaller and that of surface waters only noticeable in 2002. The recirculation seems to be largest at and south of 79° N and clearly weakens northwards, as is seen from the meridional sections. This supports the assumption that the strong recirculation area is located south of 81–82° N as already suggested by Rudels (1987). Fahrbach et al. (2001) report a recirculation of 2.6 ± 0.1 Sv just east of 0° E between 78.50° N and 79° N, so we are likely to miss some of the recirculation through the north-south section having it located at 0° meridian. Almost 50 % of the Atlantic water entering the strait from the south recirculates as has previously been estimated by e.g. Rudels (1987), Bourke et al. (1987) and Manley (1995).

The north-south section is also located in the vicinity of a semi-permanent topographically trapped eddy of 60 km in diameter near the Molloy Deep (Wadhams and Squire,1983; Bourke et al., 1987; Johannessen et al., 1987), which causes the flow near 79°30′ N and 3° E to be westward north of the eddy and eastward south of it. In 1997 and 2003 the westward transports between 79°30′ N and 80° N, are smaller than elsewhere and in 2001 eastward.

The circulation around Yermak Plateau is similar to that obtained by Marnela et al. (2008) for the 2002 data. There is northward flow of AW in the east. The results also support the southward flow along Yermak Plateau's eastern flank (Fig. 3).

There are large differences in the heat/temperature and freshwater transports during the different years. The results are nevertheless reasonable. The net heat/temperature transport across the southern sections is, except in 1997, in the range of the transports found from direct current measurements (Schauer et al., 2004, 2008). The smaller transports through the northern sections indicate that a substantial heat loss occurs just north of 79° N.

The transport of liquid freshwater 60 mSv in 2004 and 50 mSv in 2002 and less in the earlier years is almost as large as the ice export (Dickson et al., 2007) and somewhat smaller than estimated by Rabe et al. (2009). The difference between the northern and southern sections shows that a large part of the freshwater is added to the water column just north of Fram Strait, largely in the area between the sections, mainly through ice melt.

The results presented in tables 2 and 3 imply that when the waters inside the box are warm more heat is carried northward and more heat is being used to melt sea ice inside the box. Across 79° N the freshwater transport is largest (smallest) when the volume transport is largest (smallest). This might be interpreted as the salinity of low-salinity surface water having low year to year (summer) variance.

In the deep and in the intermediate waters below the density surface 28.06 there is a net southward transport at 79° N of 0.6 Sv in 1984, 0.5 Sv in 1997, 0.7 Sv in 2002 and 0.1 Sv northward in 2004. The mean of the 4 yr equals 0.4 Sv net southward transport, a single value that was used as one constraint on the deep exchanges in the earlier work on the transports through single sections at 79° N (Rudels et al., 2008), and suggests that such constraint on single sections might be realistic.

The method used here is rather simple. It requires only the use of hydrographic data with constraints. The individual northward and southward transports obtained for heat (temperature) and freshwater are somewhat arbitrary, due to the choice of reference

OSD
9, 3127–3190, 2012

temperature and salinity but also due to the limited number of stations available which allows for some smaller scale features to pass unnoticed. The results for the net transports through Fram Strait as well as for the heat lost and freshwater formed between the sections, however, are comparable to those from more sophisticated methods.

Acknowledgements. This work has received support from the European Union through the 6th framework programme DAMOCLES (Contract No 018509) and from the Academy of Finland (no 210551). Roberta Pirazzini and Timo Vihma are warmly thanked for the help with the ECMWF ERA Interim data and the related computations.

References

Aagaard, K. and Carmack, E. C.: The role of sea ice and other fresh water in the Arctic circulation, J. Geophys. Res., 94, 14485–14498, 1989.

Aagaard, K. and Greisman, P.: Toward new mass and heat budgets for the Arctic Ocean, J. Geophys. Res., 80, 3821–3827, 1975.

Aagaard, K., Darnall, C., and Greisman, P.: Year-long current measurements in the Greenland-Spitsbergen Passage, Deep Sea Res., 20, 743–746, 1973.

Beszczynska-Möller, A., Fahrbach, E., Schauer, U., and Hansen, E.: Variability in Atlantic water temperature and transport at the entrance to the Arctic Ocean, 1997–2010, ICES J. Mar. Sci., 69, 852–863, doi:10.1093/icesjms/fss056, 2012.

Bourke, R. H., Tunnicliffe, M. D., Newton, J. L., Paquette, R. G., and Manley, T. O.: Eddy near the Molloy Deep revisited, J. Geophys. Res., 92, 6773–6776, 1987.

Bourke, R. H., Weigel, A. M., and Paquette, R. G.: The westward turning branch of the West Spitsbergen Current, J. Geophys. Res., 93, 14065–14077, 1988.

Carmack, E. C., Macdonald, R. W., Perkin, R. G., McLaughlin, F. A., and Pearson, R. J.: Evidence for warming of Atlantic water in the Southern Canadian Basin of the Arctic Ocean: results from the Larsen-93 expedition, Geophys. Res. Lett., 22, 1061–1064, doi:10.1029/95GL00808, 1995.

Dickson, R., Rudels, B., Dye, S., Karcher, M., Meincke, J., and Yashayaev, I.: Current estimates of freshwater flux through Arctic and subarctic seas, Prog. Oceanogr., 73, 210–230, doi:10.1016/j.pocean.2006.12.003, 2007.

de Steur, L., Hansen, E., Gerdes, R., Karcher, M., Fahrbach, E., and Holfort, J.: Freshwater fluxes in the East Greenland Current: a decade of observations, Geophys. Res. Lett., 36, L23611, doi:10.1029/2009GL041278, 2009.

Fahrbach, E., Meincke, J., Østerhus, S., Rohardt, G., Schauer, U., Tverberg, V., and Verduin, J.: Direct measurements of volume transports through Fram Strait, Polar Res., 20, 217–224, 2001.

Fieg, K., Gerdes, R., Fahrbach, E., Beszczynska-Möller, A., and Schauer, U.: Simulation of oceanic volume transports through Fram Strait 1995–2005, Ocean Dynam., 60, 491–502, doi:10.1007/s10236-010-0263-9, 2012.

Foldvik, A., Aagaard, K., and Tørresen, T.: On the velocity field of the East Greenland Current, Deep Sea Res., 35, 1335–1354, 1988.

Gascard, J.-C., Kergomard, C., Jeannin, P.-F., and Fily, M.: Diagnostic study of the Fram Strait marginal ice zone during summer from 1983 and 1984 marginal ice zone experiment Lagrangian observations, J. Geophys. Res., 93, 3613–3641, 1988.

Holfort, J., Hansen, E., Østerhus, S., Dye, S., Jónsson, S., Meincke, J., Mortensen, J., and Meredith, M.: Freshwater Fluxes East of Greenland, in: Arctic-subarctic Ocean Fluxes, edited by: Dickson, R. R., Meincke, J., and Rhines, P., Springer, Dordrecht, 263–287, 2008.

Houssais, M.-N., Rudels, B., Friedrich, H., and Quadfasel, D.: Exchanges through Fram Strait, in: Nordic Seas Symposium on the Results of the Greenland Sea Project (GSP) 1987–1993, Extended Abstracts, edited by: Meincke, J., Hamburg, 87–91, 1995.

Jacobsen, J. P. and Jensen, A. J. C.: Examination of hydrographical measurements from the research vessels Explorer and Dana during the summer of 1924, Rap. Proces., 39, 31–84, 1926.

Johannessen, J. A., Johannessen, O. M., Svendsen, E., Shuchman, R., Manley, T., Campbell, W. J., Josberger, E. G., Sandven, S., Gascard, J. C., Olaussen, T., Davidson, K., and Van Leer, J.: Mesoscale eddies in the Fram Strait marginal ice zone during the 1983 and 1984 marginal ice zone experiments, J. Geophys. Res., 92, 6754–6772, 1987.

Karcher, M. J., Gerdes, R., Kauker, F., and Köberle, C.: Arctic warming: evolution and spreading of the 1990s warm event in the Nordic seas and the Arctic Ocean, J. Geophys. Res., 108, 3034, doi:10.1029/2001JC001265, 2003.

Karcher, M., Gerdes, R., and Kauker, F.: Long-term variability of atlantic water inflow to the Northern Seas: insights from model experiments, in: Arctic-Subarctic Ocean Fluxes, edited by: Dickson, R. R., Meincke, J., and Rhines, P., Springer, Dordrecht, 111–130, 2008.

OSD
9, 3127–3190, 2012

Recirculation and transports in Fram Strait

M. Marnela et al.

Title Page
Abstract | Introduction
Conclusions | References
Tables | Figures
◀| |▶
◀ ▶
Back | Close
Full Screen / Esc
Printer-friendly Version
Interactive Discussion

Klenke, M. and Schenke, H. W.: A new bathymetric model for the central Fram Strait, Mar. Geophys. Res., 23, 367–378, doi:10.1023/A:1025764206736, 2002.
Manley, T. O.: Branching of Atlantic water within the Greenland-Spitsbergen passage: an estimate of recirculation, J. Geophys. Res., 100, 20627–20634, 1995.
Marnela, M., Rudels, B., Olsson, K. A., Anderson, L. G., Jeansson, E., Torres, D. J., Messias, M. J., Swift, J. H., and Watson, A. J.: Transports of Nordic Seas water masses and excess SF_6 through Fram Strait to the Arctic Ocean, Prog. Oceanogr., 78, 1–11, 2008.
Maslowski, W., Marble, D., Walczowski, W., Schauer, U., Clement, J. L., and Semtner, A. J.: On climatological mass, heat, and salt transports through the Barents Sea and Fram Strait from a pan-Arctic coupled ice-ocean model simulation, J. Geophys. Res., 109, C03032, doi:10.1029/2001JC001039, 2004.
Melling, H., Agnew, T. A., Falkner, K. K., Greenberg, D. A., Lee, C. M., Münchow, A., Petrie, B., Prinsenberg, S. J., Samuelson, R. M., and Woodgate, R. A.: Fresh-water fluxes via Pacific and Arctic outflows across the Canadian Polar Shelf, in: Arctic-Subarctic Ocean Fluxes, edited by: Dickson, R. R., Meincke, J., and Rhines, P., Springer, Dordrecht, 193–247, 2008.
Padman, L. and Erofeeva, S.: A barotropic inverse tidal model for the Arctic Ocean, Geophys. Res. Lett., 31, L02303, doi:10.1029/2003GL019003, 2004.
Palfrey Jr., K. M.: Physical oceanography of the northern part of the Greenland Sea in the summer of 1964, MS thesis, University of Washington, Seattle, 63 pp., 1967.
Polyakov, I. V., Beszczynska, A., Carmack, E., Dmitrenko, I., Fahrbach, E., Frolov, I. E., Gerdes, R., Hansen, E., Holfort, J., Ivanov, V. V., Johnson, M. A., Karcher, M., Kauker, F., Morison, J., Orvik, K. A., Schauer, U., Simmons, H. L., Skagseth, Ø., Sokolov, V. T., Steele, M., Timokhov, L. A., Walsh, D., and Walsh, J. E.: One more step toward a warmer Arctic, Geophys. Res. Lett., 32, L17605, doi:10.1029/2005GL023740, 2005.
Quadfasel, D., Gascard, J.-C., and Koltermann, K.-P.: Large-scale oceanography in Fram Strait during the 1984 marginal ice zone experiment, J. Geophys. Res., 92, 6719–6728, 1987.
Quadfasel, D., Sy, A., Wells, D., and Tunik, A.: Warming in the Arctic, Nature, 350, 385, doi:10.1038/350385a0, 1991.
Rabe, B., Schauer, U., Mackensen, A., Karcher, M., Hansen, E., and Beszczynska-Möller, A.: Freshwater components and transports in the Fram Strait – recent observations and changes since the late 1990s, Ocean Sci., 5, 219–233, doi:10.5194/os-5-219-2009, 2009.
Rudels, B.: On the mass balance of the Polar Ocean, with special emphasis on the Fram Strait, Norsk Polarinst. Skri., 188, 53 pp., 1987.

OSD
9, 3127–3190, 2012

Recirculation and transports in Fram Strait

M. Marnela et al.

Rudels, B., Marnela, M., and Eriksson, P.: Constraints on estimating mass, heat and freshwater transports in the Arctic Ocean: an exercise, in: Arctic-Subarctic Ocean Fluxes, edited by: Dickson, R. R., Meincke, J., and Rhines, P., Springer, Dordrecht, 315–341, 2008.

Schauer, U., Fahrbach, E., Østerhus, S., and Rohardt, G.: Arctic warming through the Fram Strait: oceanic heat transports from 3 years of measurements, J. Geophys. Res., 109, C06026, doi:10.1029/2003JC001823, 2004.

Schauer, U., Beszczynska-Möller, A., Walczowski, W., Fahrbach, E., Piechura, J., and Hansen, E.: Variation of measured heat flow through the fram strait between 1997 and 2006, in: Arctic-Subarctic Ocean Fluxes, edited by: Dickson, R. R., Meincke, J., and Rhines, P., Springer, Dordrecht, 65–85, 2008.

Schlichtholz, P. and Houssais, M. N.: An inverse modeling study in Fram Strait, Part I: dynamics and circulation, Deep-Sea Res., 46, 1083–1135, 1999.

Schlichtholz, P. and Houssais, M.-N.: An overview of the θ-S correlations in Fram Strait based on the MIZEX 84 data, Oceanologia, 44, 243–272, 2002.

Skagseth, Ø., Drinkwater, K. F., and Terrile, E.: Wind- and buoyancy-induced transport of the Norwegian Coastal Current in the Barents Sea, J. Geophys. Res., 116, C08007, doi:10.1029/2011JC006996, 2011.

Smedsrud, L. H., Ingvaldsen, R., Nilsen, J. E. Ø., and Skagseth, Ø.: Heat in the Barents Sea: transport, storage, and surface fluxes, Ocean Sci., 6, 219–234, doi:10.5194/os-6-219-2010, 2010.

Teigen, S. H., Nilsen, F., Skogseth, R., Gjevik, B., and Beszczynska-Möller, A.: Baroclinic instability in the West Spitsbergen Current, J. Geophys. Res., 116, C07012, doi:10.1029/2011JC006974, 2011.

Untersteiner, N.: On the mass and heat budget of Arctic sea ice, Arch. Meteorol. Geophys. Bioklim., 12, 151–182, 1961.

Wadhams, P. and Squire, V. A.: An ice-water vortex at the edge of the East Greenland Current, J. Geophys. Res., 88, 2770–2780, 1983.

Wessel, P. and Smith, W. H. F.: New, improved version of Generic Mapping Tools released, EOS T. Am. Geophys. U., 79, p. 579, doi:10.1029/98EO00426, 1998.

Table 1. Baroclinic volume transports (Sv) from zonal sections (no constraints applied). At 79° N section positive transports are northward/into the box, at the northern section positive transports are southward/into the box.

		79° N		North		
Year	Nwrd	swrd	net	Nwrd	swrd	net
1984	7.77	−9.20	−1.43	−3.45	8.37	4.92
1997	3.85	−7.94	−4.09	−4.01	8.69	4.68
2002	9.54	−13.97	−4.44	−3.08	6.78	3.70
2004	8.31	−9.82	−1.51	−4.25	9.01	4.76
mean	7.37	−10.23	−2.86	−3.70	8.21	4.52
std	2.13	2.26	1.40	0.46	0.86	0.48

OSD
9, 3127–3190, 2012
Recirculation and transports in Fram Strait
M. Marnela et al.

Table 2. Transports from zonal sections with constraints applied. At 79° N section positive transports are northward/into the box, at the northern section positive transports are southward/into the box. **(a)** Volume transports (Sv), **(b)** Heat/temperature transports (TW) relative to a varying reference temperature, **(c)** Freshwater transports (mSv) relative to a varying reference salinity.

a)		79° N		North		
Year	Nwrd	swrd	net	Nwrd	swrd	net
1984	7.83	−10.00	−2.17	−5.22	7.36	2.14
1997	4.12	−8.37	−4.25	−4.14	8.38	4.24
2002	9.89	−14.01	−4.13	−3.03	7.10	4.07
2004	8.66	−10.48	−1.82	−6.05	7.81	1.76
mean	7.62	−10.72	−3.09	−4.60	7.66	3.05
std	2.15	2.06	1.10	1.14	0.49	1.11

b)		79° N			North		
Year	Ref T	Nwrd	swrd	net	Nwrd	swrd	net
1984	1.141	34.2	8.8	43.1	3.6	−21.9	−18.3
1997	0.389	16.6	−2.0	14.7	4.2	−14.3	−10.1
2002	0.817	33.8	1.9	35.7	5.2	−26.6	−21.3
2004	1.089	33.1	−5.0	28.1	6.2	−31.9	−25.7
mean	0.861	29.4	0.9	30.4	4.8	−23.7	−18.9
std	0.294	7.4	5.2	10.5	1.0	6.4	5.7

c)		79° N			North		
Year	Ref S	Nwrd	swrd	net	Nwrd	swrd	net
1984	34.756	−53.4	−8.1	−61.6	−10.6	34.7	24.2
1997	34.650	−10.7	−8.4	−19.0	4.5	6.5	11.0
2002	34.672	−34.6	−44.5	−79.1	15.5	5.3	20.7
2004	34.752	−24.8	−42.0	−66.7	11.6	−5.6	6.0
mean	34.710	−30.9	−25.7	−56.6	5.2	10.2	15.5
std	0.045	15.6	17.5	22.6	9.9	14.9	7.3

Table 3. Water mass definitions.

Water masses	Density Range	Nordic Seas water masses	Arctic Ocean water masses
Surface layer	$\sigma_\theta < 27.70$	warm Surface Water (wSW)	Polar Surface Water (PSW)
Atlantic layer	$27.70 \leq \sigma_\theta < 27.97$	Atlantic Water (AW)	Arctic Atlantic Water (AAW)
Intermediate layer I	$27.97 \leq \sigma_\theta$, $\sigma_{0.5} < 30.444$, $\theta > 0$	dense Atlantic Water (dAW) S & θ decreasing with depth	dense Arctic Atlantic Water (dAAW) S increasing, θ decreasing with depth.
Intermediate layer II	$27.97 \leq \sigma_\theta$, $\sigma_{0.5} < 30.444$, $\theta \leq 0$	Arctic Intermediate Water (AIW) upper S & θ decreasing with depth, lower S & θ increasing with depth	upper Polar Deep Water (uPDW) S increasing, θ decreasing with depth.
Deep Water I	$30.444 \leq \sigma_{0.5}$, $\sigma_{1.5} < 35.142$	Nordic Seas Deep Water I (NDWI), $S < 34.915$	Canadian Basin Deep Water (CBDW)
Deep Water II	$35.142 \leq \sigma_{1.5}$	Nordic Seas Deep Water II (NDWII), $S < 34.915$	Eurasian Basin Deep Water (EBDW)

OSD
9, 3127–3190, 2012

Table 4. Volume, heat and freshwater transports by water masses from zonal section pairs. ThN (ThS)/SN (SS) = volume mean temperature/salinity of the northward (southward) flowing water mass.

Year	Water	Volume (Sv)			Heat (TW)					Freshwater (mSv)				
		nw	sw	net	ThN	ThS	nw	sw	net	SN	SS	nw	sw	net
							Northern section							
1984	Surf w	−0.78	1.24	0.46	0.79	−0.04	1.1	−6.0	−4.9	33.23	32.97	−35.3	65.4	30.0
	AW	−1.62	1.38	−0.24	2.62	2.26	−9.8	6.4	−3.45	34.96	34.93	9.9	−7.1	2.8
	dAW	−1.22	1.87	0.65	0.98	0.81	0.8	−2.5	−1.73	34.96	34.94	7.3	−10.2	−2.9
	Int. w	−0.69	1.55	0.86	−0.33	−0.33	4.1	−9.4	−5.2	34.92	34.91	3.2	−7.2	−3.9
	DWI	−0.49	0.93	0.44	−0.70	−0.71	3.7	−7.1	−3.4	34.92	34.92	2.4	−4.4	−2.1
	DWII	−0.42	0.38	−0.04	−0.97	−0.95	3.6	−3.3	0.4	34.92	34.92	2.0	−1.8	0.2
1997	Surf w	−0.75	1.77	1.02	−1.56	−1.50	6.0	−13.7	−7.7	33.77	33.64	−19.4	52.9	33.5
	AW	−1.48	2.20	0.73	1.42	1.29	−6.2	8.1	1.9	34.85	34.84	8.9	−12.6	−3.7
	dAW	−0.76	1.81	1.06	0.54	0.50	−0.5	0.8	0.4	34.91	34.90	5.7	−13.6	−7.8
	Int. w	−0.42	1.46	1.05	−0.31	−0.29	1.2	−4.1	−2.9	34.91	34.91	3.2	−11.1	−8.0
	DWI	−0.27	0.61	0.34	−0.71	−0.69	1.2	−2.7	−1.5	34.92	34.92	2.2	−4.9	−2.7
	DWII	−0.47	0.52	0.05	−0.91	−0.90	2.5	−2.8	−0.2	34.93	34.93	3.9	−4.3	−0.4
2002	Surf w	−0.28	1.40	1.13	−1.75	−1.70	2.9	−14.5	−11.6	34.34	33.68	−2.7	41.1	38.4
	AW	−1.15	1.80	0.65	1.54	1.08	−3.4	1.9	−1.5	34.87	34.83	6.5	−8.5	−1.9
	dAW	−0.68	1.50	0.82	0.79	0.59	0.1	−1.4	−1.3	34.92	34.91	5.1	−10.5	−5.4
	Int. w	−0.38	1.54	1.15	−0.40	−0.31	1.9	−7.1	−5.2	34.90	34.90	2.6	−10.4	−7.8
	DWI	−0.21	0.46	0.25	−0.84	−0.65	1.4	−2.8	−1.3	34.91	34.92	1.5	−3.4	−1.9
	DWII	−0.33	0.39	0.07	−0.92	−0.90	2.3	−2.8	−0.5	34.92	34.93	2.4	−3.0	−0.6
2004	Surf w	−0.91	1.01	0.09	1.89	−1.02	−3.0	−8.7	−11.7	34.22	33.99	−14.3	22.7	8.5
	AW	−1.87	1.99	0.12	2.43	1.40	−10.3	2.6	−7.8	34.93	34.85	9.7	−5.7	3.9
	dAW	−0.79	1.48	0.69	0.64	0.47	1.4	−3.8	−2.3	34.92	34.90	3.9	−6.5	−2.7
	Int. w	−0.68	1.78	1.11	−0.35	−0.30	4.0	−10.1	−6.1	34.91	34.90	3.1	−8.1	−4.9
	DWI	−0.71	0.87	0.17	−0.69	−0.65	5.2	−6.2	−1.1	34.92	34.92	3.5	−4.4	−0.9
	DWII	−1.10	0.68	−0.42	−0.89	−0.89	8.9	−5.5	3.4	34.92	34.93	5.6	−3.6	2.0

OSD
9, 3127–3190, 2012

OSD
9, 3127–3190, 2012

Table 4. Continued.

Year	Water	Volume (Sv)			Heat (TW)					Freshwater (mSv)				
		nw	sw	net	ThN	ThS	nw	sw	net	SN	SS	nw	sw	net
						Southern section								
1984	Surf w	0.77	−1.31	−0.54	5.79	0.59	14.7	2.9	17.6	34.92	33.23	−3.7	−58.7	−62.4
	AW	3.41	−2.51	0.90	3.33	2.64	30.7	−15.4	15.3	35.05	34.99	−29.3	17.3	−12.1
	dAW	1.96	−3.09	−1.13	1.31	1.17	1.4	−0.4	1.0	34.98	34.97	−12.9	19.4	6.5
	Int. w	0.91	−1.89	−0.98	−0.45	−0.40	−5.9	12.0	6.0	34.90	34.91	−4.0	8.4	4.4
	DWI	0.40	−0.86	−0.46	−0.80	−0.75	−3.2	6.6	3.5	34.91	34.91	−1.8	4.0	2.2
	DWII	0.39	−0.35	0.04	−1.01	−0.98	−3.5	3.1	−0.4	34.91	34.91	−1.8	1.6	−0.2
1997	Surf w	0.77	−1.70	−0.92	2.15	−0.28	5.6	4.7	10.3	33.84	33.45	18.5	−60.5	−41.9
	AW	1.48	−2.16	−0.68	2.71	2.03	14.1	−14.6	−0.4	34.98	34.92	−14.5	17.5	3.0
	dAW	0.76	−1.75	−0.99	1.00	0.75	1.9	−2.6	−0.7	34.94	34.92	−6.4	13.9	7.5
	Int. w	0.60	−2.10	−1.50	−0.52	−0.45	−2.2	7.2	5.0	34.89	34.90	−4.3	15.5	11.2
	DWI	0.50	−0.64	−0.15	−0.93	−0.81	−2.7	3.2	0.5	34.91	34.91	−3.8	5.0	1.2
	DWII	0.01	−0.02	−0.00	−1.04	−0.94	−0.1	0.1	0.0	34.91	34.92	−0.1	0.1	0.0
2002	Surf w	1.67	−2.91	−1.24	3.45	0.45	18.1	4.4	22.4	33.94	33.14	36.2	−132.0	−95.8
	AW	3.08	−3.35	−0.27	3.08	2.54	28.7	−23.7	5.0	35.01	34.96	−31.0	28.5	−2.5
	dAW	2.44	−3.58	−1.14	1.03	0.92	2.1	−1.5	0.6	34.96	34.95	−20.6	29.3	8.7
	Int. w	1.60	−2.58	−0.98	−0.37	−0.36	−7.8	12.5	4.7	34.91	34.91	−11.2	18.1	6.9
	DWI	0.69	−1.17	−0.48	−0.74	−0.70	−4.4	7.3	2.9	34.92	34.92	−5.0	8.5	3.5
	DWII	0.41	−0.42	−0.01	−0.91	−0.89	−2.9	3.0	0.0	34.92	34.92	−3.0	3.1	0.1
2004	Surf w	1.28	−2.32	−1.04	3.34	0.77	11.8	3.0	14.9	34.10	33.45	24.8	−89.4	−64.7
	AW	4.08	−3.73	0.34	3.30	2.89	37.0	−27.6	9.4	35.03	34.99	−33.2	26.5	−6.8
	dAW	1.27	−1.91	−0.64	0.85	0.66	−1.2	3.4	2.1	34.93	34.92	−6.8	9.3	2.6
	Int. w	0.97	−1.73	−0.76	−0.41	−0.35	−6.0	10.2	4.2	34.90	34.90	−4.4	7.8	3.4
	DWI	0.52	−0.60	−0.08	−0.79	−0.72	−4.0	4.5	0.5	34.91	34.92	−2.5	2.9	0.5
	DWII	0.55	−0.19	0.36	−0.92	−0.89	−4.5	1.6	−3.0	34.92	34.92	−2.7	0.9	−1.8

Table 5. Volume transports (Sv) (positive westward) from the meridional (north-south) sections with constraints applied.

Year	1997	2001	2003	
Latitude	78.8–80° N	78.8–80° N	78–78.8° N	78.8–80° N
Surface water	0.14	−0.00	0.11	0.29
Atlantic water	0.37	0.06	0.70	0.50
Dense AW	0.19	−0.02	0.41	0.28
Intermediate w.	0.04	−0.19	−0.03	0.08
Deep water I	−0.02	−0.07	−0.01	−0.04
Deep water II	0.02	0.05	0.02	−0.02
Net	0.74	−0.17	1.20	1.09

OSD
9, 3127–3190, 2012

Table 6. Volume transports (Sv) (positive westward) from the meridional sections with no constraints applied ($v = 0$ at the bottom).

	78–78.8° N			78.8–80° N		
Year	westward	eastward	net	westward	eastward	net
1997	2.56	−1.87	0.69	1.80	−1.14	0.66
2001	2.31	−1.34	0.97	2.10	−2.67	−0.57
2003	2.61	−1.55	1.06	1.89	−0.65	1.23

OSD
9, 3127–3190, 2012

Table 7. 2004 volume transports of a surface layer at 35 to 425 m depth divided to about 5° sections from ADCP velocities taken at every 0.25° and from geostrophy with constraints applied. Transports are positive northward and negative southward for both northern and 79° N section.

Longitude	−12 . . . −10		−10 . . . −5		−5 . . . 0		0 . . . 5		5 . . . 10		10 . . . 12	
range (°)	ADCP	geostr	ADCP	geostr	ADCP	geostr	ADCP	geostr	ADCP	geostr	ADCP	geostr
North nwrd	0.01	0.11	0.25	0.14	0.15	0.15	0.32	0.13	0.51	1.27	0.09	0.56
North swrd	−0.37	−0.11	−0.69	−0.41	−0.26	−0.15	−0.12	−0.16	−0.48	−1.44	−0.07	−0.04
North net	−0.36	−0.01	−0.44	−0.28	−0.11	−0.01	0.21	−0.03	0.03	−0.17	0.02	0.52
79° N nwrd	0.13	0.05	0.27	0.32	1.24	1.07	2.35	2.14	1.46	0.63	–	–
79° N swrd	−0.22	−0.07	−1.14	−0.73	−2.48	−2.01	−2.38	−1.17	−0.89	−0.54	–	–
79° N net	−0.09	−0.02	−0.86	−0.41	−1.24	−0.93	−0.03	0.97	0.57	0.09	–	–

OSD
9, 3127–3190, 2012

Table 8a. Heat and freshwater (fw) convergence/divergence from hydrographic and ERA Interim data, with varying averages as reference temperature and salinity.
Heat lost by the ocean and heat input from the atmosphere between the two zonal sections as compared with the heat required to balance the freshwater transport via ice melt.

Year	1. Heat req. to balance fw transport	2. Oceanic heat loss	3. Heat input from atm. (ECMWF data)	2 + 3
1984	13 TW	25 TW	12 TW	37 TW
1997	3 TW	5 TW	11 TW	16 TW
2002	20 TW	14 TW	16 TW	30 TW
2004	21 TW	2 TW	16 TW	18 TW

OSD
9, 3127–3190, 2012

Table 8b. Heat and freshwater (fw) convergence/divergence from hydrographic and ERA Interim data, with varying averages as reference temperature and salinity.
Freshwater. Precipitation and evaporation from the ERA Interim data are computed for an area with ice concentration less than 90 %.

Year	1. Divergence of fw possible from oceanic heat loss	2. Sea ice melt possible from ECMWF atm. fluxes	3. P	4. E	5. P + E per time × area	1 + 2 + 5	fw divergence
1984	72 mSv	35 mSv	0.053 m	−0.010 m	0.6 mSv	108 mSv	37 mSv
1997	13 mSv	32 mSv	0.058 m	−0.009 m	1.2 mSv	46 mSv	8 mSv
2002	42 mSv	47 mSv	0.053 m	+0.002 m	1.6 mSv	90 mSv	58 mSv
2004	7 mSv	47 mSv	0.062 m	+0.002 m	1.9 mSv	56 mSv	61 mSv

OSD
9, 3127–3190, 2012

Table 9. Net volume transports at 79° N from zonal sections and from Rudels et al. (2008). Full section and from 6° W to 9° E.

	Whole section	6° W–9° E	Whole section Rudels et al. (2008)	6° W–9° E based on Rudels et al. (2008)
All years (av.)	3.1	2.7	2.7 (1.7*)	2.1
1984	2.2	2.0	1.0	0.8
1997	4.2	4.2	4.1	4.1
2002	4.1	3.4	3.6	–
2004	1.8	1.1	2.1	1.5

* Computed as a mean of 16 summer sections taken between 1980 and 2005, and then modified with budget considerations.

Discussion Paper | Discussion Paper | Discussion Paper | Discussion Paper

OSD

9, 3127–3190, 2012

Recirculation and transports in Fram Strait

M. Marnela et al.

Table 10. Volume transports (Sv) as obtained from combinations of constraints. At 79° N section positive transports are northward/into the box, at the northern section positive transports are southward/into the box. **(a)** constraints 1, 2, 5 and where applicable 6 applied. **(b)** constraints 1, 5 and where appl. 6 are applied. **(c)** constraint 5 and where appl. 6 is applied. **(d)** constraint 1 is applied. **(e)** constraints 2 and 3 are applied.

a)		79° N		North		
Year	Nwrd	swrd	net	Nwrd	swrd	net
1984	7.60	−9.90	−2.30	−5.12	7.38	2.26
1997	3.59	−8.26	−4.67	−3.99	8.65	4.66
2002	9.73	−13.68	−3.95	−2.98	6.86	3.88
2004	7.65	−10.75	−3.10	−5.25	8.30	3.04
mean	7.14	−10.65	−3.50	−4.33	7.80	3.46
std	2.22	1.97	0.89	0.92	0.71	0.90

b)		79° N		North		
Year	Nwrd	swrd	net	Nwrd	swrd	net
1984	7.30	−10.45	−3.14	−4.54	7.66	3.12
1997	3.54	−8.32	−4.79	−3.95	8.73	4.78
2002	9.66	−13.78	−4.12	−2.90	6.95	4.05
2004	7.49	−10.94	−3.45	−5.06	8.46	3.40
mean	7.00	−10.87	−3.87	−4.11	7.95	3.84
std	2.20	1.95	0.64	0.80	0.70	0.64

OSD
9, 3127–3190, 2012

Recirculation and transports in Fram Strait

M. Marnela et al.

Table 10. Continued.

c) Year	Nwrd	79° N swrd	net	North Nwrd	swrd	net
1984	7.77	−9.20	−1.43	−3.97	8.26	4.28
1997	3.85	−7.94	−4.09	−3.74	9.04	5.30
2002	9.54	−13.97	−4.44	−2.99	6.82	3.82
2004	8.31	−9.82	−1.51	−4.19	9.10	4.91
mean	7.37	−10.23	−2.87	−3.72	8.31	4.58
std	2.13	2.26	1.40	0.45	0.92	0.57

d) Year	Nwrd	79° N swrd	net	North Nwrd	swrd	net
1984	7.35	−10.31	−2.96	−4.43	7.37	2.94
1997	3.76	−8.05	−4.29	−4.20	8.49	4.29
2002	9.66	−13.79	−4.13	−2.95	7.01	4.06
2004	7.84	−10.41	−2.57	−5.44	7.97	2.53
mean	7.15	−10.64	−3.49	−4.25	7.71	3.45
std	2.14	2.05	0.74	0.89	0.57	0.74

e) Year	Nwrd	79° N swrd	net	North Nwrd	swrd	net
1984	7.92	−9.15	−1.23	−3.84	7.75	3.92
1997	4.22	−7.70	−3.48	−4.81	8.17	3.37
2002	9.93	−13.64	−3.71	−3.11	6.46	3.35
2004	8.87	−9.57	−0.71	−5.74	7.79	2.05
mean	7.74	−10.01	−2.28	−4.37	7.54	3.17
std	2.15	2.20	1.33	0.99	0.65	0.69

OSD
9, 3127–3190, 2012

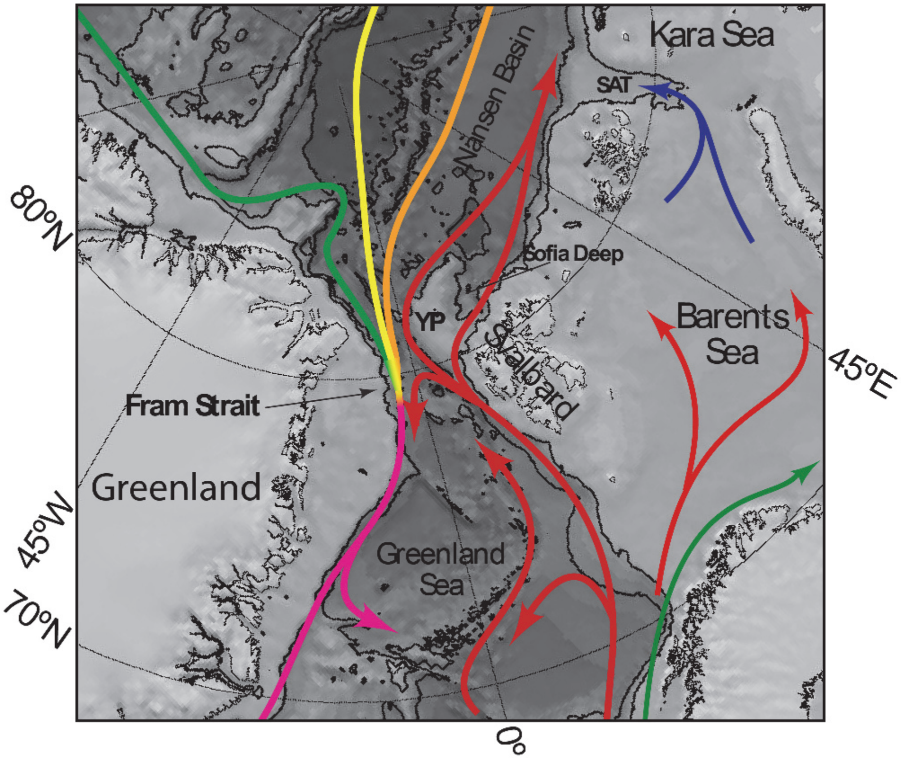

Fig. 1. Fram Strait bathymetry and AW circulation. YP = Yermak Plateau, SAT = Saint Anna-Trough.

OSD
9, 3127–3190, 2012

Recirculation and transports in Fram Strait

M. Marnela et al.

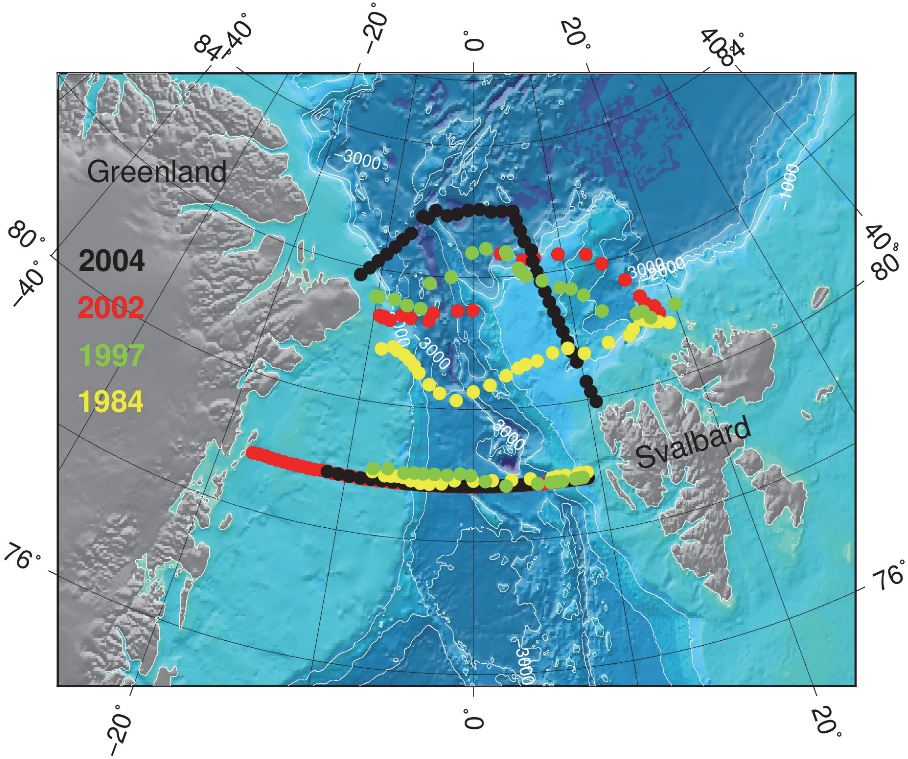

Fig. 2. Fram Strait bathymetry (IBCAO) with 1984, 1997, 2002 and 2004 stations. Map produced with GMT (Wessel and Smith, 1998).

OSD
9, 3127–3190, 2012

Title Page
Abstract | Introduction
Conclusions | References
Tables | Figures
◀| | |▶
◀ | ▶
Back | Close
Full Screen / Esc
Printer-friendly Version
Interactive Discussion

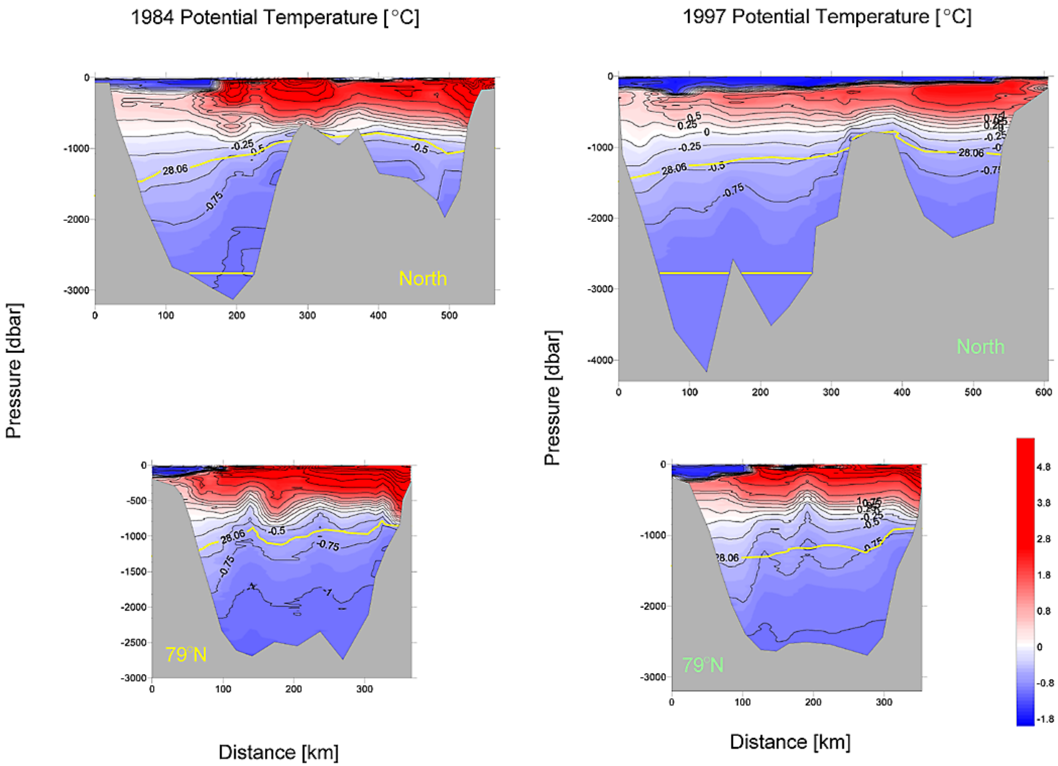

Fig. 3. Potential temperature, salinity and velocity from the zonal sections in 1984, 1997, 2002 and 2004 and from the meridional sections in 1997, 2001 and 2003 showing the constraint boundaries (yellow lines).

OSD
9, 3127–3190, 2012

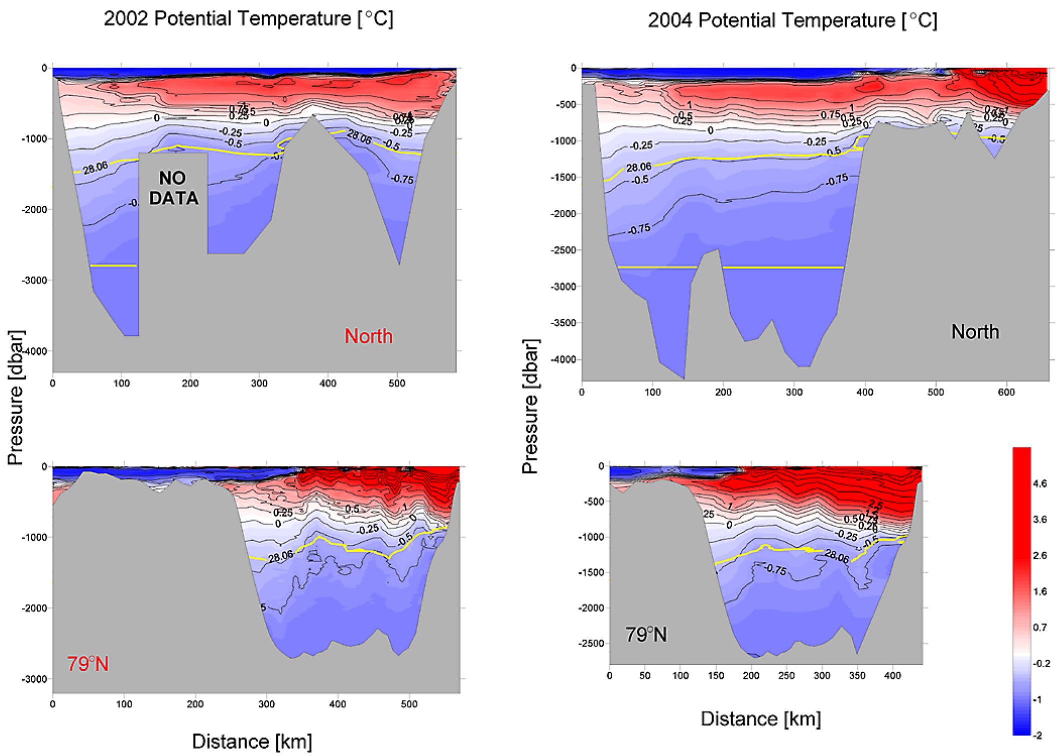

Fig. 3. Continued.

OSD

9, 3127–3190, 2012

Recirculation and transports in Fram Strait

M. Marnela et al.

Title Page
Abstract | Introduction
Conclusions | References
Tables | Figures
◂◂ | ▸▸
◂ | ▸
Back | Close
Full Screen / Esc
Printer-friendly Version
Interactive Discussion

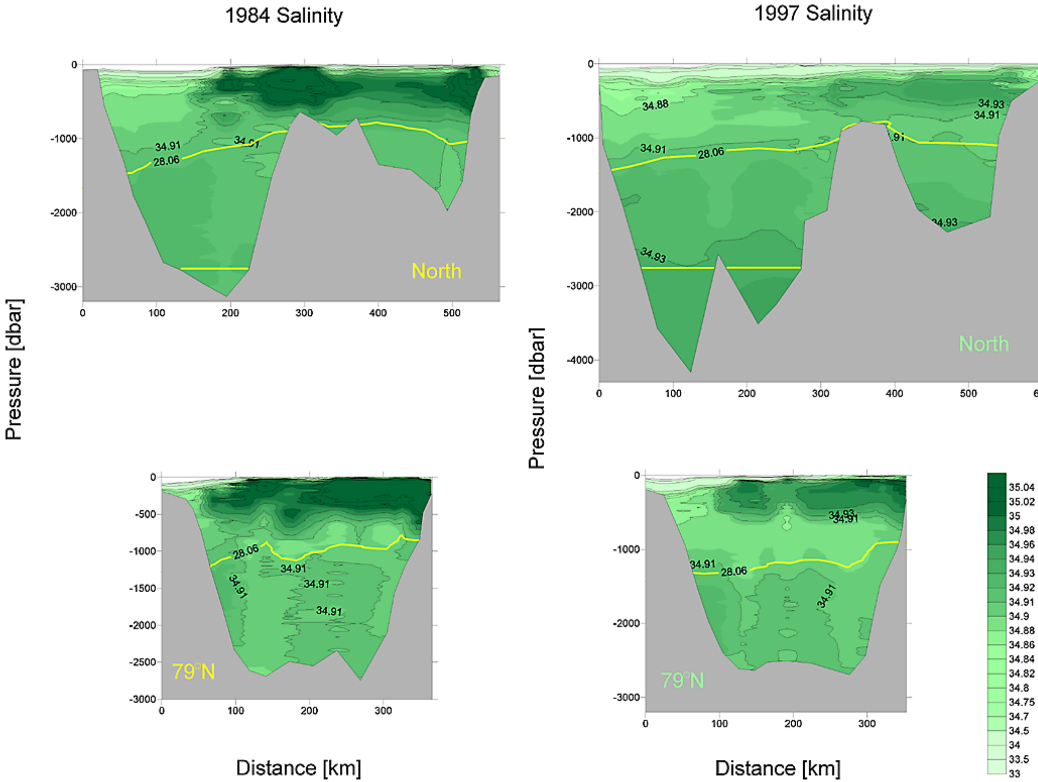

Fig. 3. Continued.

OSD
9, 3127–3190, 2012

Recirculation and transports in Fram Strait

M. Marnela et al.

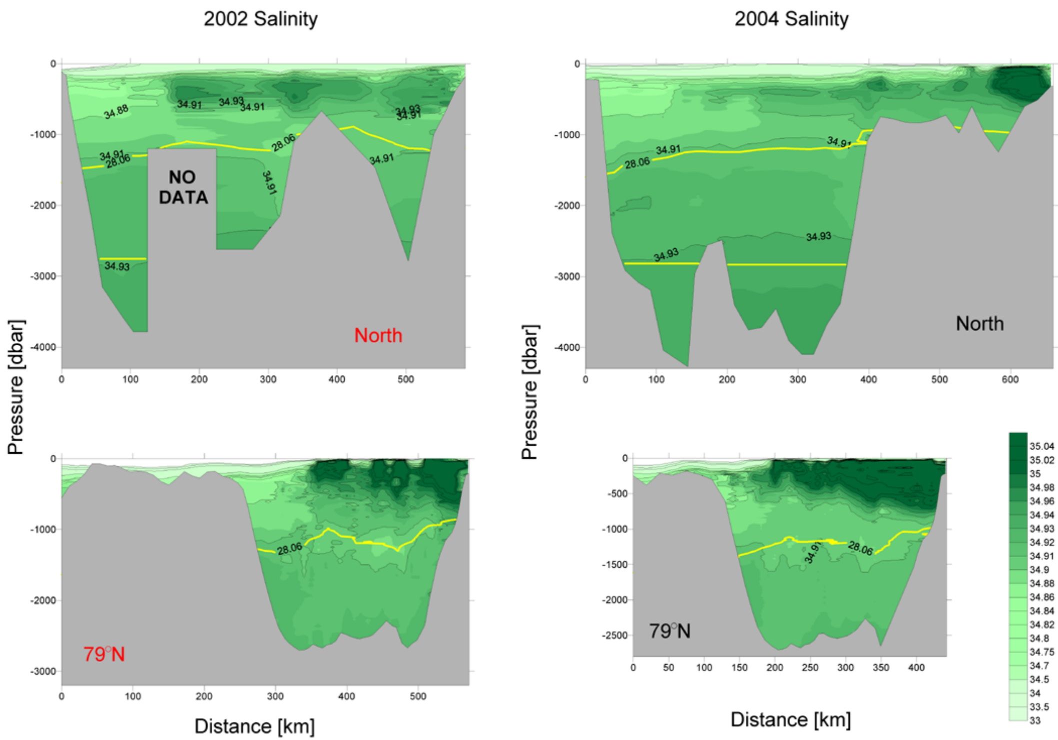

Fig. 3. Continued.

OSD
9, 3127–3190, 2012

Recirculation and transports in Fram Strait

M. Marnela et al.

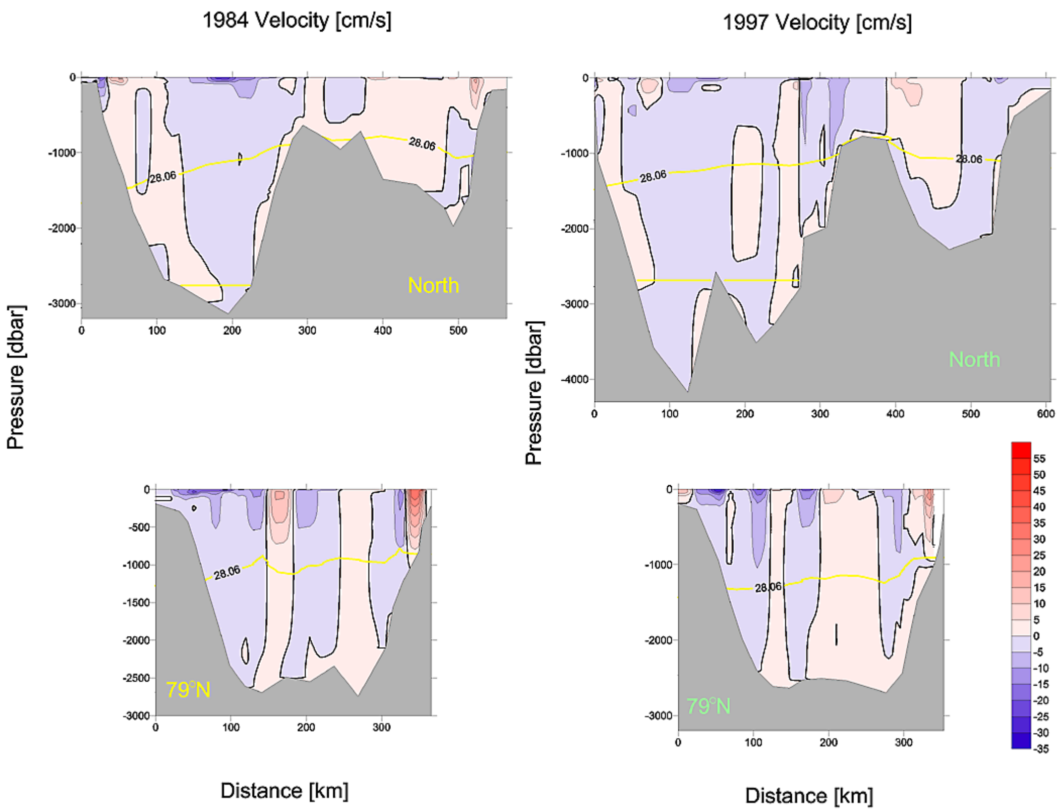

Fig. 3. Continued.

OSD
9, 3127–3190, 2012

Recirculation and transports in Fram Strait

M. Marnela et al.

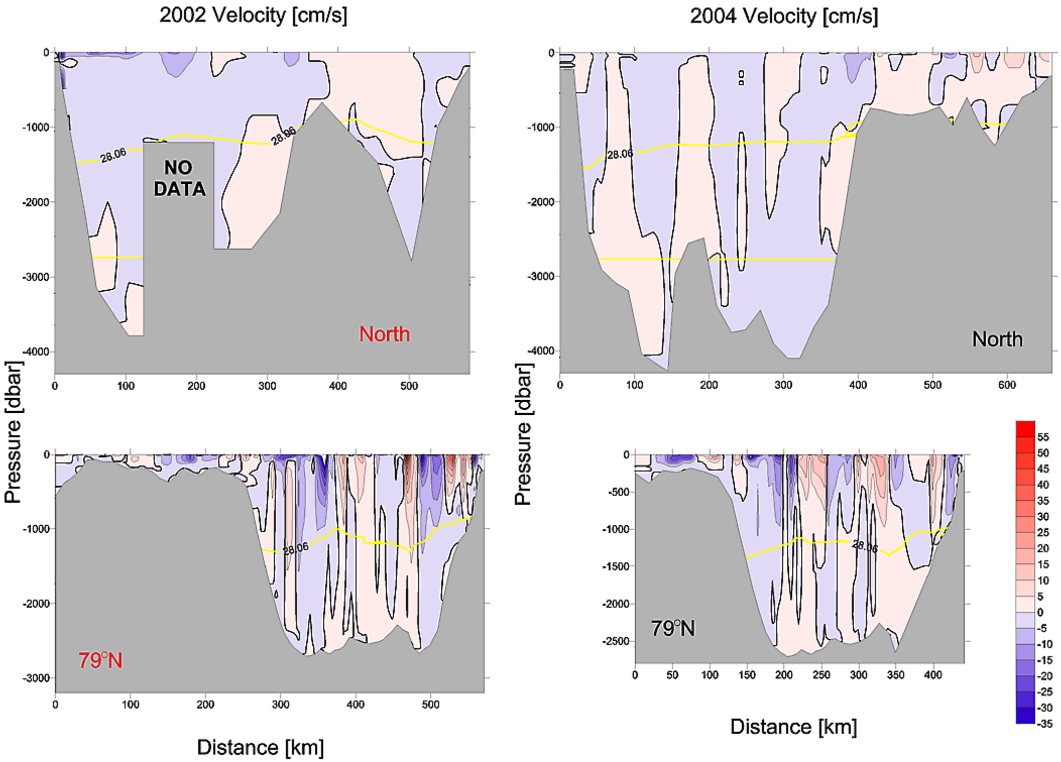

Fig. 3. Continued.

OSD
9, 3127–3190, 2012

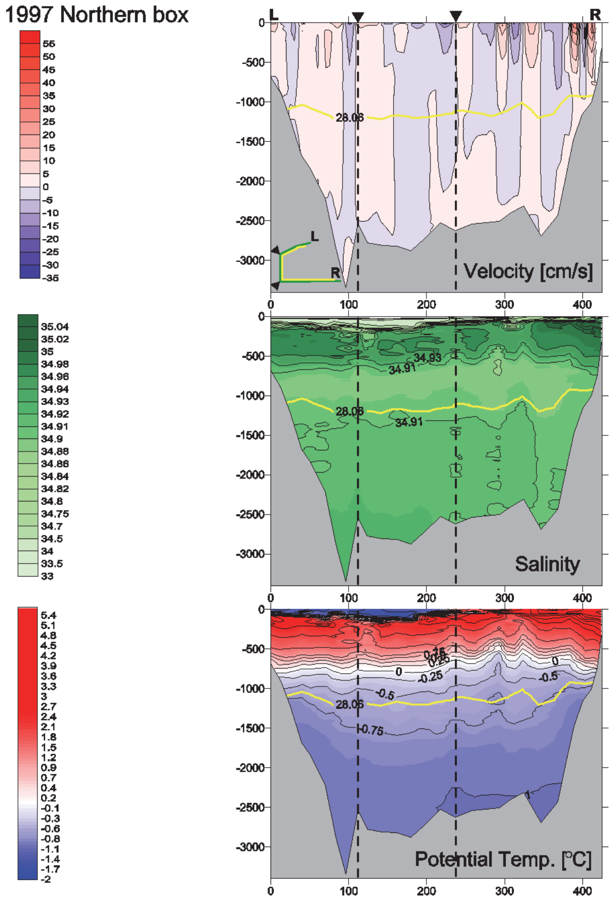

Fig. 3. Continued.

Discussion Paper | Discussion Paper | Discussion Paper | Discussion Paper |

OSD

9, 3127–3190, 2012

Recirculation and transports in Fram Strait

M. Marnela et al.

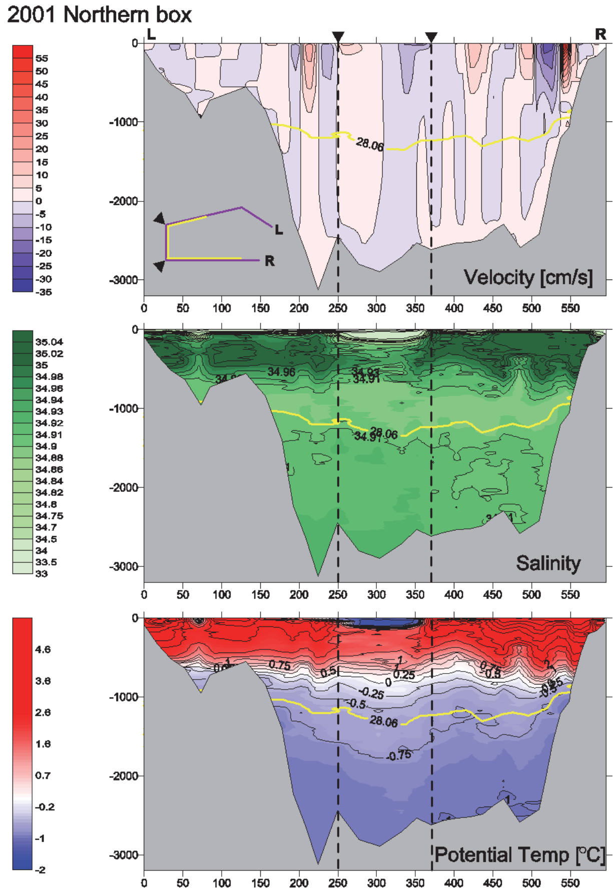

Fig. 3. Continued.

OSD
9, 3127–3190, 2012

Recirculation and transports in Fram Strait

M. Marnela et al.

Title Page
Abstract | Introduction
Conclusions | References
Tables | Figures
◀| |▶
◀ ▶
Back | Close
Full Screen / Esc
Printer-friendly Version
Interactive Discussion

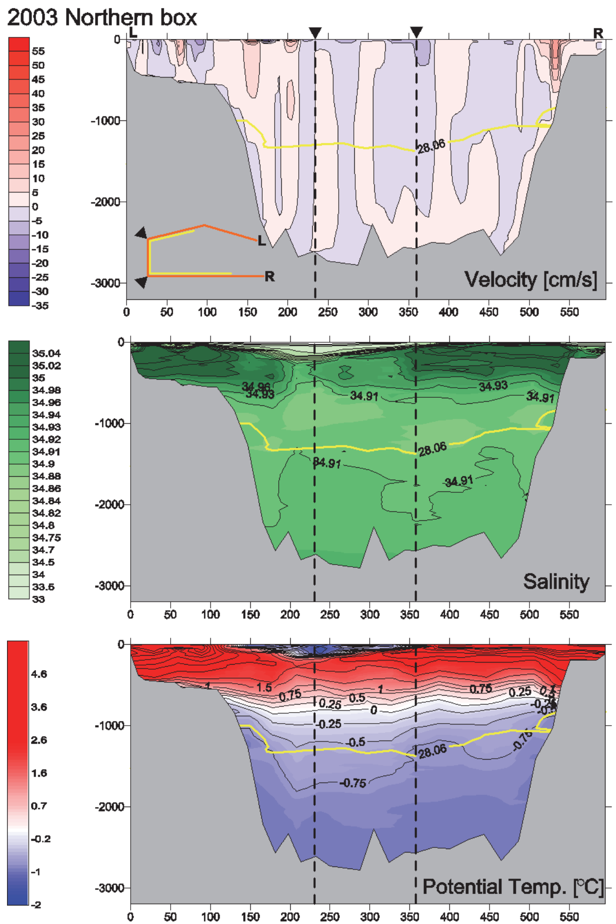

Fig. 3. Continued.

OSD
9, 3127–3190, 2012

Recirculation and transports in Fram Strait

M. Marnela et al.

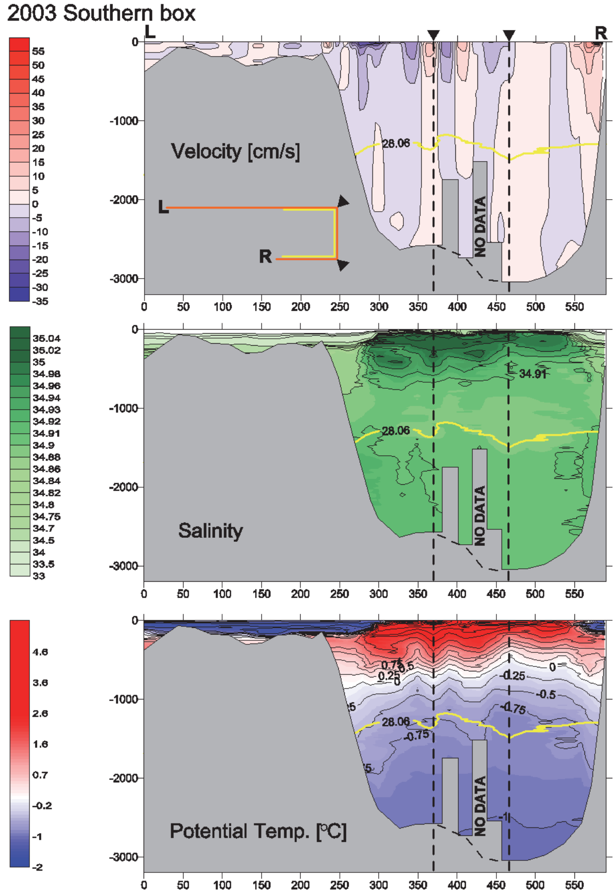

Fig. 3. Continued.

OSD
9, 3127–3190, 2012

Recirculation and transports in Fram Strait

M. Marnela et al.

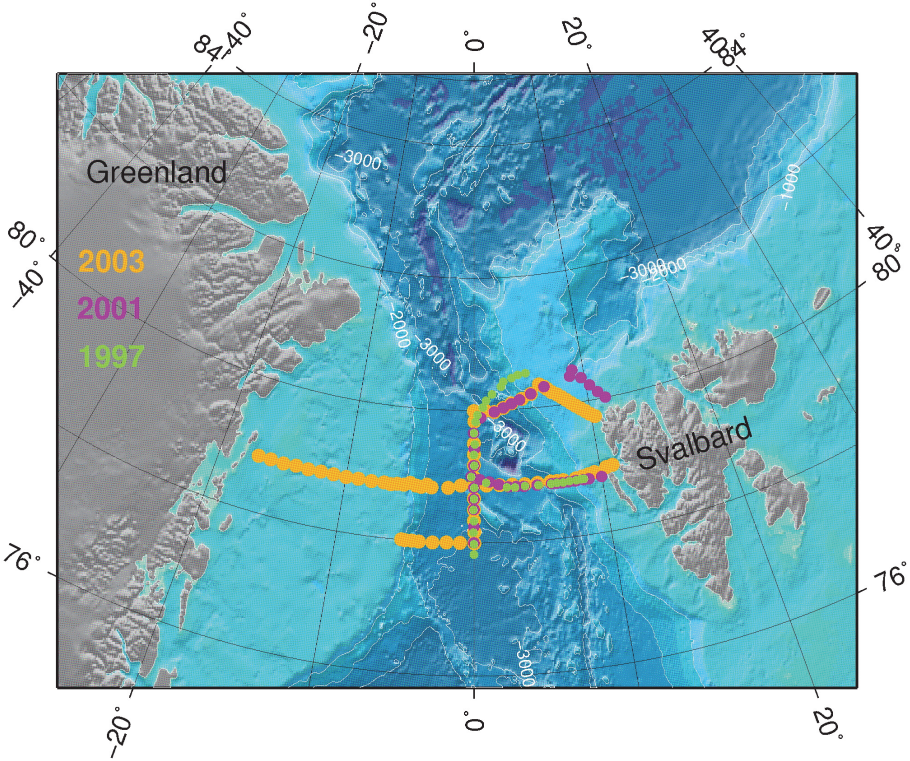

Fig. 4. Fram Strait bathymetry with 1997, 2001 and 2003 stations. Map produced with GMT (Wessel and Smith, 1998).

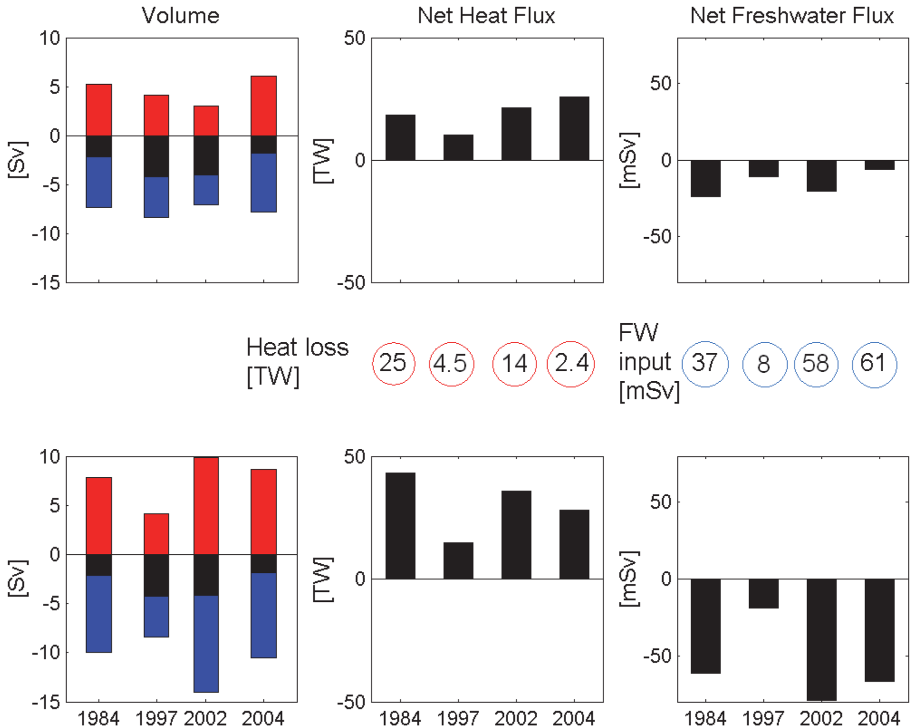

Fig. 5. Transports of volume (red northward, blue southward, black net) of the whole water column and the net heat and freshwater fluxes relative to the mean temperature and salinity of the total transports through the two sections in each year.

OSD
9, 3127–3190, 2012

Recirculation and transports in Fram Strait

M. Marnela et al.

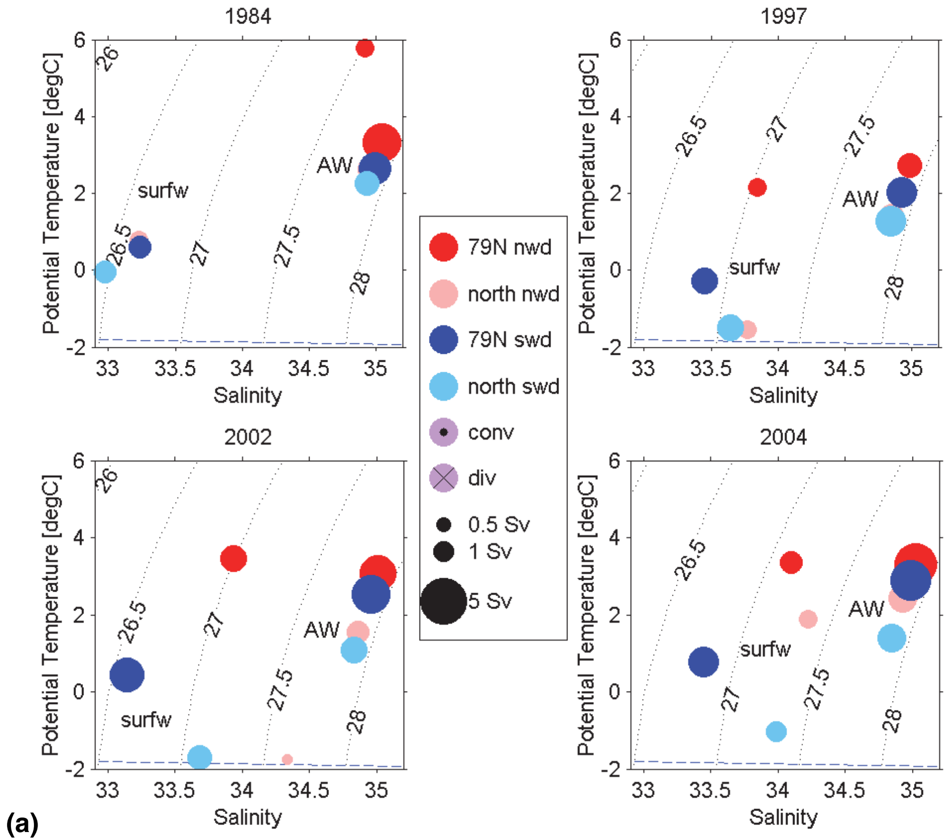

Fig. 6. *θS* volume diagrams with mean potential temperatures and salinities for different water masses for each year as well as the divergence or convergence of each water mass. The changes in volume flux are indicated by changes in the size of the circles between inflow and outflow. The water masses shown are **(a)** surface water (surfw) and AW, **(b)** AW and dAW, **(c)** intermediate (IW) and deep waters (DWI and DWII).

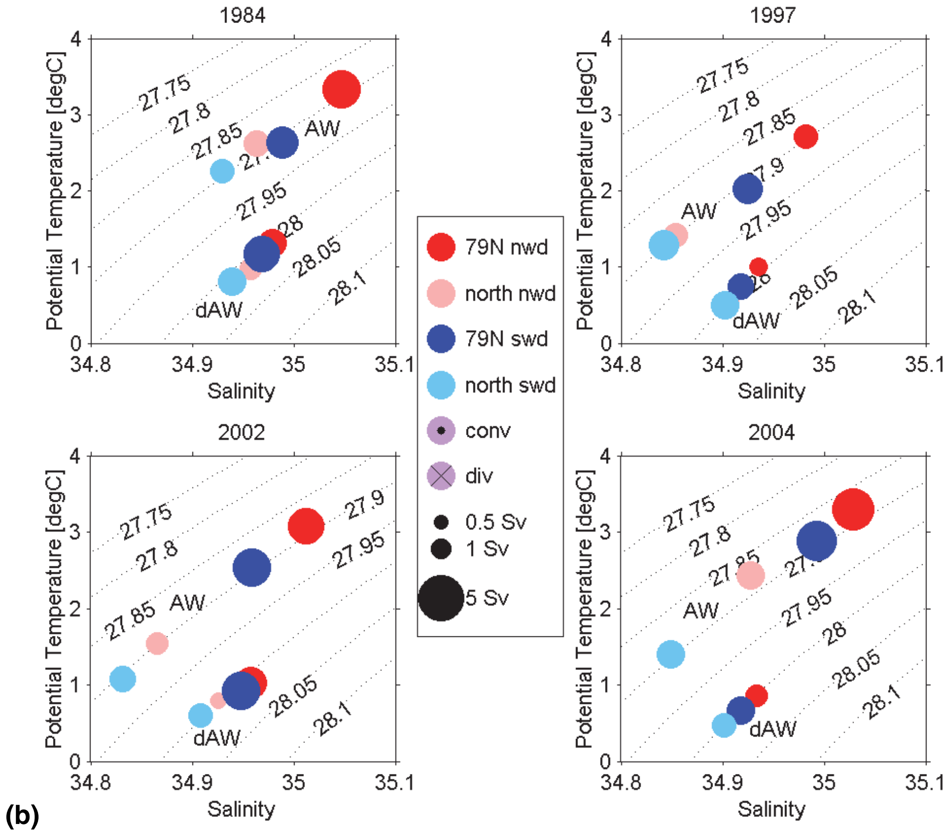

Fig. 6. Continued.

OSD
9, 3127–3190, 2012

Recirculation and transports in Fram Strait

M. Marnela et al.

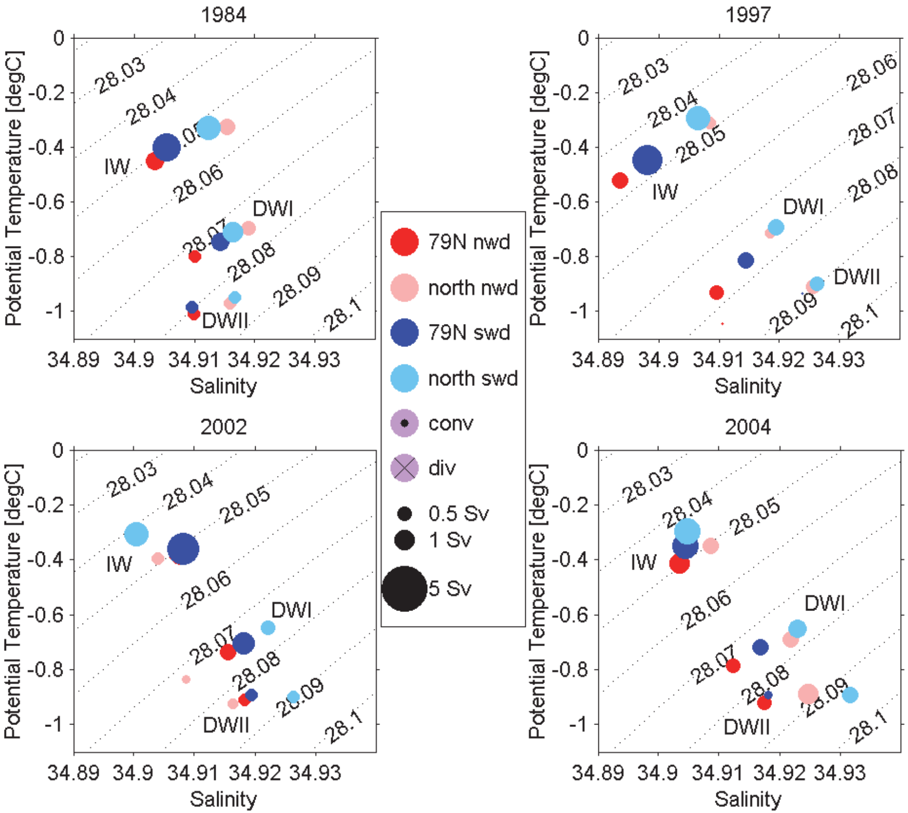

(c)

Fig. 6. Continued.

Discussion Paper | Discussion Paper | Discussion Paper | Discussion Paper |

OSD

9, 3127–3190, 2012

Recirculation and transports in Fram Strait

M. Marnela et al.

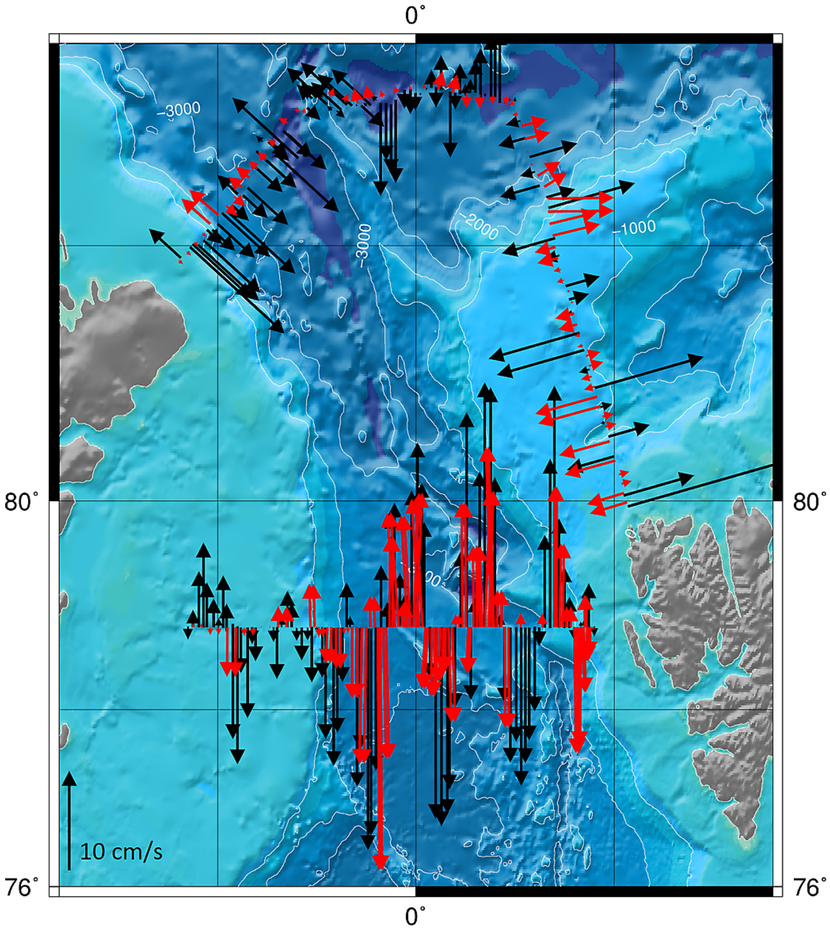

Fig. 7. Velocity vectors at approximately 160 m depth from geostrophy with constraints (red) and vessel mounted ADCP at 0.25° intervals (black) with only the velocity component in the direction of geostrophy shown. Map produced with GMT (Wessel and Smith, 1998).

OSD

9, 3127–3190, 2012